HHS Public Access

Author manuscript

Nat Neurosci. Author manuscript; available in PMC 2014 June 01.

Published in final edited form as:

Nat Neurosci. 2013 December ; 16(12): 1783–1793. doi:10.1038/nn.3559.

Opposite actions of alcohol on tonic $GABA_A$ receptor currents mediated by nNOS and PKC activity

Joshua S Kaplan[1], **Claudia Mohr**[1], and **David J Rossi**[1]

[1]Department of Behavioral Neuroscience, Oregon Health & Science University, Portland, Oregon, USA

Abstract

The molecular mechanisms that mediate genetic variability in response to alcohol are unclear. We find that alcohol has opposite actions (enhancement or suppression) on $GABA_A$ receptor ($GABA_AR$) inhibition in granule cells (GCs) of the cerebellum from behaviorally sensitive, low-alcohol consuming Sprague Dawley rats and DBA/2 mice and behaviorally insensitive, high-alcohol consuming C57BL/6 mice, respectively. The impact of alcohol on GC $GABA_AR$ inhibition is determined by a balance between two opposing effects: enhanced presynaptic vesicular release of GABA via alcohol inhibition of nitric oxide synthase (NOS), and a direct suppression of the activity of postsynaptic $GABA_ARs$. The balance of these two processes is determined by differential expression of neuronal NOS (nNOS) and postsynaptic PKC activity, both of which vary across rodent genotypes. These findings identify opposing molecular processes that differentially control the magnitude and polarity of $GABA_AR$ responses to alcohol across rodent genotypes.

Introduction

Alcohol abuse is a leading cause of preventable death and illness, and the economic cost of alcohol abuse is estimated to be $185 billion annually in the USA alone[1]. Adoption and twin studies suggest that alcohol use disorders (AUDs) are 50-60% genetically determined[2,3]. A growing body of research indicates that genetic differences in cerebellar processing and cerebellar responses to alcohol contribute to susceptibility to AUDs[2,4-6], but the mechanisms by which the cerebellum influences the development of AUDs are not known.

Insight into cerebellar contributions to AUD risk comes from studies of the low level of response (LLR) to EtOH phenotype, which is defined as requiring a higher dose of alcohol (EtOH) to achieve a given effect. EtOH-induced static ataxia (body sway), a form of cerebellar-dependent motor impairment, consistently shows LLR in individuals with a

Corresponding Author: David J Rossi, Department of Behavioral Neuroscience, Oregon Health & Science University, 3181 SW Sam Jackson Park Road, Portland, OR 97239 –HRC5B, Phone: 503-418-2685, rossid@ohsu.edu.

Author Contributions: J.S.K. and D.J.R. designed the experiments. J.S.K performed the electrophysiology experiments and C.M. performed the immunocytochemistry experiments. J.S.K and D.J.R. analyzed the data and wrote the manuscript.

Competing interests statement: The authors declare that they have no competing financial interests.

family history of AUDs compared to individuals without a family history of AUDs[5,6]. Thus, low cerebellar sensitivity to EtOH may be a risk factor for AUDs. In support of this contention, the magnitude of EtOH-induced ataxia shows an inverse relationship with EtOH consumption and preference in some inbred strains of mice[7,8] as well as lines of rodents selected for differences in EtOH consumption[9,10] or in EtOH-induced motor impairment[11]. Importantly, cerebellar specific injections of various drugs can inhibit systemically administered EtOH induced-ataxia[12], clearly indicating the central role of the cerebellum in mediating EtOH-induced ataxia.

Cerebellar granule cells (GCs) are the main integrators/processors of afferent input to the cerebellar cortex, making them powerful targets for pharmacological modulation of cerebellar processing[13,14]. GCs exhibit traditional phasic $GABA_AR$-mediated inhibitory postsynaptic currents (IPSCs), as well as the more recently discovered tonic form of $GABA_AR$ inhibition, mediated by extrasynaptic, $\alpha_6\delta$ subunit containing $GABA_ARs$[14-18]. The tonic form of $GABA_AR$ inhibition mediates 75% of total GC $GABA_AR$ inhibition, thereby powerfully controlling signal transmission through the cerebellar cortex[14]. Both the frequency of spontaneous GABAergic IPSCs (sIPSCs) and the magnitude of the tonic $GABA_AR$-mediated current are enhanced by behaviorally relevant concentrations of EtOH[19,20]. Therefore, genetic variation in the sensitivity of GC $GABA_AR$ inhibition to EtOH is a candidate mechanism for mediating the relationship between cerebellar LLR and AUD in humans, or high EtOH consumption in animal models. Unfortunately, almost all research on EtOH-induced potentiation of GC $GABA_AR$ inhibition has been done on Sprague-Dawley rats (SDRs), and little attention has been given to how the sensitivity of GC $GABA_AR$ inhibition to EtOH varies across species or divergent genotypes[21]. This neglect is a significant problem because SDRs have a high sensitivity, low EtOH consumption phenotype[22], and thus may not be as relevant to AUD in humans.

We report here that EtOH can either increase or decrease $GABA_AR$ mediated inhibition of GCs, and the net impact across populations of GCs shifts, in a graded fashion, from strong enhancement in high sensitivity, low EtOH consuming rodents to suppression in low sensitivity, high EtOH consuming rodents. Furthermore, we found that the net impact of EtOH on GC $GABA_AR$ inhibition is determined by a balance between enhanced vesicular release of GABA (via EtOH inhibition of nitric oxide synthase (NOS)) and a direct suppression of $GABA_ARs$. The balance of these two processes is determined by differential expression of neuronal NOS (nNOS) and levels of postsynaptic PKC activity, both of which vary across rodent genotypes. These findings substantially alter the current dogma that the primary action of EtOH on $GABA_AR$ transmission is potentiation. Instead, our data indicate that EtOH can potentiate or suppress $GABA_AR$ transmission, and the polarity varies across rodent genotypes with divergent EtOH-related behavioral phenotypes.

Results

Mouse GC tonic current mediated by extrasynaptic $GABA_ARs$

To determine if EtOH consumption phenotype is associated with differences in GC $GABA_AR$ sensitivity to EtOH, we made voltage-clamp recordings (Vh = -60mV, with ECl= ~ 0mV, see methods) from GCs in cerebellar slices obtained from alcohol naïve,

prototypical high and low EtOH consuming mice, C57BL/6J (B6) and DBA/2J (D2) mice respectively[7]. First, we characterized the basal properties of $GABA_AR$-mediated inhibition in GCs from these two strains of mice. Similar to the well characterized SDR GCs, B6 and D2 GCs exhibit phasic sIPSCs and a powerful tonic current (tonic current amplitude= B6: 26.74 ± 4.27 pA; D2: 22.90 ± 2.64 pA, *n* = 12 cells from 5 animals each; see Supplementary Fig. 1 for current measuring methodology), both mediated by $GABA_ARs$ as evidenced by their blockade by the $GABA_AR$ antagonist, GABAzine (10μM, Fig. 1a,g). The GC tonic $GABA_AR$ current is thought to be mediated by extrasynaptic $GABA_ARs$ containing the α6 and δ subunit[14-16,18], but this has not been fully established in B6 GCs and has not been examined at all in D2 GCs. We used confocal microscopy to examine B6 and D2 cerebellar slices immunostained with antibodies to the $GABA_AR$ α6 and δ subunit, and found that both subunits are richly and exclusively expressed by GCs in both strains of mice, particularly on their dendritic terminals (Fig. 1b α6; 1d δ). Furthermore, in both strains of mice, the tonic current was reduced by furosemide (100μM, at which concentration it is specific for $GABA_ARs$ containing the α6 subunit[14,23]; Fig. 1c,g, furosemide block of current= B6: 17.24 ± 2.16 pA; D2: 13.99 ± 1.75 pA, *n* = 17 cells each), and was enhanced by the $GABA_AR$ agonist THIP (500nM, which at concentrations up to 1μM is specific for $GABA_ARs$ containing δ subunits[16]; Fig. 1e,g, THIP induced current= B6: 45.41 ± 3.93 pA, *n* = 18; D2: 33.67 ± 7.40 pA, *n* = 10 cells). Finally, diazepam (300nM), which potentiates the response of α1 containing receptors, but not α6 containing receptors, and does not affect the tonic $GABA_AR$ current in SDR GCs[14,24], did not affect the tonic $GABA_AR$ current in D2 or B6 mouse GCs (Fig. 1f,g;, D2: -0.08 ± 0.34 pA, *n* = 9 cells from 3 animals, *P* = .82; B6: -0.39 ± 0.57 pA, *n* = 7 cells from 2 animals, *P* = 0.52, one-sample *t*-tests). In the same cells, diazepam increased the magnitude and decay time of sIPSCs (Supplementary Fig. 2), confirming its efficacy at diazepam-sensitive synaptically located α1 containing $GABA_ARs$. These data indicate that, similar to previous reports in SDR GCs, both B6 and D2 GCs exhibit tonic $GABA_AR$ currents mediated by extrasynaptic α6δ-containing receptors. There were no detectable differences between B6 and D2 GC $GABA_AR$ mediated tonic currents or sIPSCs (Fig. 1g **and** Supplementary Fig. 2, all *P* > 0.05).

Opposite actions of EtOH on GC tonic $GABA_AR$ currents

Bath application of EtOH to SDR cerebellum increases the frequency of GC sIPSCs and the magnitude of the tonic $GABA_AR$ current (Fig. 2a)[19,20]. Similar to SDR GCs, in some B6 and D2 GCs, bath application of 52mM EtOH caused an increase in the frequency of sIPSCs and an associated potentiation of the tonic $GABA_AR$ current (Fig. 2b,e). However, in 41-45% of both B6 (16/39 cells) and D2 (14/31 cells) GCs, EtOH had no discernible effect on the tonic current (Fig. 2c,e) or the frequency of sIPSCs (discussed in greater detail below). Surprisingly, in 44% of B6 (17/39 cells) GCs and in 10% of D2 GCs (3/31 cells), EtOH actually suppressed the tonic $GABA_AR$ current (Fig. 2d,e). Importantly, EtOH did not affect the holding current in any species of GC when $GABA_ARs$ were blocked by GABAzine (10μM, D2: *n* = 8 cells from 3 animals, B6: n = 11 cells from 4 animals, and SDRs: n = 32 cells from 8 animals, Fig. 2f,g), confirming that EtOH-induced inward and outward currents are due to potentiation and suppression of the tonic $GABA_AR$ current respectively. To determine the overall impact on a population of GCs, and hence the output of the cerebellum (the sole output of the cerebellar cortex is via the Purkinje cell, whose

output is influenced by ~10^5 GCs[14,25]) we calculated the mean response of all cells from each type of rodent (Fig. 2h). The averaged impact of EtOH on the $GABA_AR$ tonic current for a population of neurons was significantly different between strains ($H(2) = 49.54$, $P < .001$, by Kruskal-Wallis) with the average for SDR and D2 GCs being potentiation (increase in tonic current = SDR: 4.65 ± 0.51 pA, $n = 47$ cells; D2: 2.51 ± 0.84 pA, $n = 31$ cells), whereas, the average impact on B6 GC tonic current was suppression (reduced by 2.32 ± 1.30 pA, $n = 39$ cells). Thus, 52mM EtOH will suppress transmission through the cerebellar cortex in low EtOH consuming SDRs and D2 mice, but it will enhance transmission through the cerebellar cortex in high EtOH consuming B6 mice[13,14].

Although the correspondence between GC $GABA_AR$ response phenotype and EtOH consumption phenotype is quite striking, to determine if this potential relationship is generalizable, we examined GC $GABA_AR$ responses to EtOH in the first replicate line of WSP and WSR mice (WSP1 & WSR1), which were bred for divergence in sensitivity to EtOH withdrawal phenotype but have a similar EtOH consumption phenotype that is intermediate between the low EtOH consuming D2 mice and SDRs and the high EtOH consuming B6 mice (Fig. 2i)[26]. While the GC $GABA_AR$ response to EtOH varied significantly across strains ($H(4) = 59.03$, $P < .001$, by Kruskal-Wallis), it was similar in WSP1 (reduced by 0.49 ± 1.12 pA, $n = 9$ cells from 2 animals) and WSR1 mice (reduced by 1.50 ± 1.34 pA, $n = 7$ cells from 2 animals, $P = .57$, unpaired t-test), and fell between SDR/D2 and B6 responses, being on average slightly suppressed (Fig. 2i). Thus, the net impact of EtOH on $GABA_AR$ transmission in a population of GCs varies from strong potentiation in low EtOH consuming SDRs and D2s, to strong suppression in high EtOH consuming B6s, with intermediate impact in moderate EtOH consuming WSR1 and WSP1 mice.

In the preceding experiments, we used a relatively high concentration of EtOH (52mM) to maximize our chances of discovering potentially subtle differences in responses across genotypes. However, while blood alcohol concentrations (BECs) reach 52mM in many non-choice rodent experiments (delivery of 2g/kg EtOH leads to BECs of 45-55mM, depending on species[27]), voluntary consumption of EtOH in rodents and humans more typically leads to BECs in the range of 5-25mM. To determine if the two types of response are activated by BECs achieved during voluntary EtOH consumption, we constructed dose response curves in B6 mouse and SDR GCs, which respectively exhibit predominantly suppression and exclusively enhancement (Fig. 2j,k). As reported by others[19,20], in SDR GCs, concentrations of EtOH as low as 9mM (as would be achieved in an adult human consuming two units of alcohol) significantly enhance the magnitude of tonic $GABA_AR$ currents, and the degree of enhancement dose dependently increases until plateauing at about 52mM (Fig. 2j,k; 9mM: 0.81 ± .20 pA, $n = 21$ cells; 31mM: 1.85 ± .38 pA, $n = 22$ cells; 52mM: 4.65 ± .51 pA, $n = 47$ cells; 79mM: 6.14 ± 1.29 pA, $n = 15$ cells generated from a minimum 3 animals/condition). Conversely, EtOH significantly suppresses the magnitude of tonic $GABA_AR$ current in the majority of B6 GCs, starting at 9mM and plateauing at 52mM (Fig. 2j,k; 9mM: -0.79 ± 0.19 pA, $n = 23$ cells; 31mM: -1.38 ± 0.31 pA, $n = 24$ cells; 52mM: -3.37 ± 1.46 pA, $n = 39$ cells; 79mM: -2.62 ± 0.96 pA, $n = 8$ cells generated from a minimum 3 animals/condition). The magnitude of the EtOH-induced current in both directions was

tightly and significantly correlated with the magnitude and polarity of the EtOH-induced change in noise variance (Fig. 2l; Pearson correlation, $r = 0.79$, $P < 0.001$, $n = 79$ cells from 5 SDRs, 10 D2s, and 10 B6s). Combined with the fact that EtOH does not induce any detectable currents in either direction in the presence of the $GABA_AR$ antagonist GABAzine (Fig. 2f,g), these data confirm that the EtOH-induced shifts in macroscopic current are mediated by enhancement and suppression of the opening of $GABA_AR$ receptor channels. Thus, both suppression and enhancement of $GABA_AR$-mediated tonic currents can occur in response to recreationally/clinically relevant concentrations of EtOH.

EtOH inhibition of nNOS increases Golgi cell firing

As has been shown previously in SDR GCs, blocking action potentials with TTX (500nM) abolishes EtOH-induced enhancement of GC sIPSC frequency and tonic $GABA_AR$ current (Fig. 3a,b)[19]. Thus, the increase in both sIPSCs and tonic $GABA_AR$ current are due to increased action-potential driven, vesicular GABA release from Golgi cells (the GABAergic input to GCs), but the mechanisms mediating increased Golgi cell firing are not fully understood[19,28]. Biochemical and behavioral studies have determined that EtOH inhibits cerebellar nitric oxide synthase (NOS), and the inhibition of cerebellar NOS mediates EtOH-induced ataxia[12,29], but the underlying mechanisms are not known. A recent study found that blocking NOS increases GC sIPSC frequency and tonic $GABA_AR$ current magnitude (which we confirm in Fig. 3c,d)[30], very similar to what we and others observe for the response to EtOH (Fig. 2a). We therefore reasoned that the EtOH-induced increase in $GABA_AR$ transmission may be mediated by inhibition of NOS. In support of our hypothesis, blocking NOS with the substrate inhibitor L-nitroarginine (L-NA, 300μM) significantly inhibited the EtOH-induced increase in sIPSC frequency and tonic $GABA_AR$ current in both SDRs and D2s (Fig. 3e,f, all $P < .05$). To ensure that the block by L-NA is a true pharmacological blockade of EtOH actions at NOS, and not simply occlusion of the response to EtOH due to saturation of the vesicular GABA release machinery (since blocking NOS increases vesicle release, Fig. 3c), we conducted control experiments with nicotine. Nicotine (500nM) activates Golgi cell nicotinic acetylcholine receptors, which excites Golgi cells[17], thereby increasing vesicular GABA release and resultant increases in tonic $GABA_AR$ currents (Fig. 3g). In contrast to the impact on EtOH, blocking NOS did not affect nicotine-induced increases in GC tonic $GABA_AR$ currents (Fig. 3g). Thus, the block by L-NA of EtOH-induced enhancement of IPSCs and tonic $GABA_AR$ currents is specific, and not due to occlusion by saturation of the system.

Our data suggest that EtOH-induced increases in GC IPSC frequency and tonic $GABA_AR$ current magnitude are mediated by EtOH suppression of a tonic production of NO that under control conditions limits the rate of vesicular GABA release. To further substantiate this notion, we used a fluorescent biochemical assay of cellular NO production, and tested whether NO is tonically generated in the GC layer, and whether EtOH suppresses such NO production (Fig. 4). DAF-FM diacetate is an NO-sensitive fluorophore that is cell permeant until deacetylated by intracellular esterases, resulting in its intracellular accumulation. DAF-FM is essentially non-fluorescent until it reacts with NO, whereupon its fluorescence quantum yield increases 180 fold, making it an ideal intracellular sensor of [NO]. Cerebellar slices were soaked for 30 minutes in ACSF supplemented with DAF-FM (1μM; $n = 20$

slices from 2 animals) alone, DAF-FM + the NOS antagonist, L-NA (300μM; *n* = 22 slices from 2 animals), or DAF-FM + EtOH (52mM; *n* = 20 slices from 2 animals). Slices were then fixed, and analyzed with confocal microscopy. 3-D projections of confocally acquired images of DAF-FM treated slices revealed robust fluorescence throughout the GC layer and in the white matter axon tracks innervating the GC layer (Fig. 4a). Slices treated with DAF-FM + L-NA exhibited a similar pattern of fluorescence emission, but the intensity was significantly reduced compared to DAF-FM alone ($P < 0.001$; Fig. 4b,d), confirming that the fluorescence signal is generated by NO production by NOS. EtOH (52mM) also significantly reduced the intensity of fluorescence emission without noticeably affecting the pattern ($P < 0.001$ by unpaired *t*-test; Fig. 4c,d). Thus, there is a tonic production of NO in the GC layer, and EtOH substantially inhibits that production.

Our data indicate that EtOH-induced increase in vesicular GABA release is triggered by blocking NO production, but is dependent on Golgi cell action potential (AP) firing (since it is abolished by TTX, Fig. 3a,b). This raises the question of whether EtOH block of NOS causes the increase in Golgi cell AP firing that drives increased GABA release. To test this possibility, we made current-clamp recordings of Golgi cell responses to EtOH and NOS antagonists (Fig. 5). Under control conditions, with appropriate current injection (mean = 21.8 ± 18.6 pA), Golgi cells stably fired APs (mean frequency = 0.7 ± 0.2 Hz, n = 12 cells from 4 animals; Fig. 5a,b, **top panels**). Bath application of an NOS antagonist (L-NMMA, 200μM) or EtOH (52mM) significantly increased Golgi cell AP firing frequency (L-NMMA-induced increase = 26.7 ± 6.1%, *n* = 4 cells from 2 animals; EtOH-induced increase = 53.6 ± 14.1%, *n* = 8 cells from 4 animals; Fig. 5a,b,d). Pretreatment with another NOS antagonist (L-NA, 300μM) also increased Golgi cell firing frequency, and prevented further increases by EtOH (EtOH-induced change = -10.6 ± 8.3%, *n* = 9 cells from 3 animals; Fig. 5c,d). Thus, EtOH inhibition of NO production increases Golgi cell AP firing, thereby driving EtOH-induced increases in GC IPSC frequency and tonic $GABA_AR$ current magnitude.

Collectively, our data indicate that the EtOH-induced increase in GC sIPSCs and tonic $GABA_AR$ current is driven by increased Golgi cell AP firing, consequent to EtOH suppression of basal NO production. We therefore hypothesized that lower NOS expression and consequent NO production could underlie the relative lack of potentiation of $GABA_AR$ inhibition in B6 GCs compared to SDR and D2 GCs (Fig. 2e). Accordingly, we used neuronal NOS (nNOS) immunohistochemistry and confocal microscopy to examine the expression and distribution of nNOS in SDR, D2 mouse and B6 mouse cerebellum (Fig. 6a-g). nNOS expression is widespread and confluent in the granule cell layer of the SDR and D2 cerebellum, primarily in a ring-like pattern, encircling GC nuclei stained with Hoechst (Fig. 6a,c), and in the cytoplasm of Golgi cell somas (identified by their larger size and expression of the GABA synthetic enzyme GAD65/67; Fig. 6e). Although similar ring-like staining was seen in B6 cerebellum, it was greatly restricted, and there were frequent dark patches, or lack of staining throughout the B6 GC layer (Fig. 6b), and the staining intensity in individual Golgi cell somas also appeared less intense (Fig. 6f). Importantly, nNOS signal was completely absent in slices from mice in which the nNOS gene was deleted, confirming the specificity of our antibody (Supplementary Fig. 4). Although interpreting differences in

immunostaining intensity across preparations can be problematic, given the stark qualitative differences, we developed two methods to quantify nNOS expression levels around GCs and in Golgi cell somas respectively. Since nNOS expression around GC somas appeared to reflect an all or nothing absence or presence of nNOS at various points around the GC soma perimeter, rather than a confluent difference in expression level at all points, we quantified the degree of GC encirclement. To do this, we adjusted the gain of each image to equalize peak fluorescence intensities across slices, and then calculated the degree of GC encirclement for every GC in the image (see Supplementary Fig. 3 for details). The degree of GC encirclement by nNOS staining differed between groups ($H(2) = 2290.13$, $P < .001$) and was significantly smaller in B6 slices compared to SDR and D2 slices (Fig. 6d, **both** $P < 0.001$ by Dunn's method of multiple comparisons). Conversely, since the pattern of nNOS staining in Golgi cell somas was qualitatively similar across species, but appeared less intense in B6 mouse Golgi cells, we quantified overall Golgi cell nNOS staining intensity. To reduce potential variability caused by differences in antibody penetration or light scattering across preparations we normalized nNOS staining intensity to the staining intensity of GAD 65/67 in the same cell. The ratio of the mean intensity (across the entire Golgi cell soma) of nNOS staining relative to GAD 65/67 staining is significantly smaller in B6 mouse Golgi cells compared to either D2 mouse or SDR Golgi cells (Fig. 6g; **main effect of group, $F(2,18) = 31.03$,** $P < 0.001$ by one-way ANOVA and $P < .001$ for both pairwise comparisons for SDR and D2 compared to B6). Thus, the level of nNOS expression in Golgi cell bodies, as well as in GC somas that densely surround Golgi cell somas, dendrites, and axons (Fig. 6e,f), is significantly reduced in B6 mice compared to D2 mice and SDRs. Given the diffusible nature of NO, both compartments could influence the Golgi cell target that suppresses Golgi cell AP firing, and thus the reduction in both compartments in B6 mice could explain the absence of EtOH-induced enhancement of GC sIPSCs and tonic $GABA_AR$ current (Fig. 2e,h).

To test whether the observed differences in nNOS immunostaining manifest as reduced NOS function, we used GC $GABA_AR$ current responses to pharmacological inhibition of NOS as a bioassay of NOS function (Fig. 6h-l). In keeping with reduced expression of nNOS in B6 cerebellum, blocking NOS directly, with the NOS substrate antagonist L-NMMA (200μM) produced a significantly smaller potentiation of sIPSC frequency and tonic $GABA_AR$ current in B6 GCs (increase in sIPSC frequency = 2.76 ± 7.55%; tonic current = 2.25 ± 0.47 pA, $n = 11$ cells from 4 animals) compared to SDR (increase in sIPSC frequency = 120.37 ± 53.94%; tonic current = 6.20 ± 1.39 pA, $n = 16$ cells from 7 animals) and D2 GCs (increase in sIPSC frequency = 102.47 ± 46.08%; tonic current = 4.97 ± 0.82 pA, $n = 17$ cells from 4 animals; $P < 0.05$ by Mann-Whitney U tests; Fig. 6k,l).

Although reduced expression of nNOS could alone account for the lack of physiological response to EtOH in B6 mice, another possible contribution is reduced activity of the nNOS that is expressed. To test this possibility, we treated slices with L-arginine, a rate limiting reactant in the production of NO by NOS. In SDR slices, L-arginine (100μM) enhanced EtOH-induced increases in sIPSC frequency and tonic $GABA_AR$ current magnitude (Supplementary Fig. 5a,c,d), suggesting that endogenous levels of L-arginine are rate limiting for NO production in the SDR cerebellum. In contrast, L-arginine did not affect the

actions of EtOH on $GABA_AR$ currents in B6 mice (Supplementary Fig. 5b,c,d). Taken together, the data suggest that the absence of potentiation of GC $GABA_AR$ transmission in ~85% of B6 GCs (Fig. 2e) is primarily due to a lower level of expression of nNOS, the inhibition of which mediates EtOH-induced potentiation of $GABA_AR$ transmission in SDR and D2 GCs.

Postsynaptic EtOH actions suppress tonic $GABA_AR$ currents

While differences in nNOS expression explain the relative lack of potentiation of GC $GABA_AR$ transmission in B6 GCs, it does not explain the suppression of GC $GABA_AR$ transmission observed in ~45% of B6 GCs and ~10% of D2 GCs (Fig. 2e). Since EtOH-induced potentiation of GC tonic $GABA_AR$ current is due to action-potential dependent increased vesicular release of GABA (Fig. 3a,b), we considered that suppression of the tonic current might be mediated by suppression of vesicular release of GABA. However, the sIPSC frequency was not suppressed in B6 GCs that showed EtOH-induced suppression of the tonic $GABA_AR$ current (Fig. 7a). Furthermore, blocking action potentials with TTX did not affect the EtOH-induced suppression of tonic $GABA_AR$ current in B6 GCs (Fig. 7b,c). Interestingly, in D2 GCs, TTX not only blocked the EtOH-induced potentiation of tonic $GABA_AR$ current, but it converted potentiation into suppression, similar to EtOH actions in B6 GCs (Fig. 7b,c; EtOH-induced current in TTX in SDR: 0.09 ± 0.15 pA, n = 11 cells from 6 animals; B6: 2.77 ± 1.26 pA, n = 13 cells from 3 animals; D2: 2.71 ± 1.00, n = 9 cells from 2 animals). These data indicate that EtOH can inhibit tonic $GABA_AR$ currents independent of vesicular GABA release, and inhibition is dominant in B6 GCs, absent in SDR GCs and present in D2 GCs but typically obscured by EtOH-induced increases in GABA release similar to what is observed in SDR GCs.

Suppression of tonic $GABA_AR$ currents without corresponding changes in vesicular GABA release is suggestive of a direct action of EtOH on the extrasynaptic $GABA_ARs$ that generate tonic $GABA_AR$ inhibition. However, changes in extracellular GABA concentration can occur independent of changes in vesicular release[17]. To circumvent potential actions of EtOH on GABA release or uptake mechanisms, and directly test whether EtOH suppression of tonic $GABA_AR$ currents is via direct actions in the postsynaptic cell, we conducted nucleated patch experiments, whereby the GC is extracted from the slice with the recording electrode (Fig. 7d-f). We then bath applied a low concentration of GABA (100nM, which should only activate high affinity α6/δ containing $GABA_ARs$[16]) to isolated GCs, and examined responses to EtOH. In addition to visual determination of physical isolation, we confirmed that GC somas were functionally isolated from the slice by the disappearance of tonic $GABA_AR$ currents and sIPSCs (Fig. 7d). Using this approach, for B6 GCs in which EtOH suppressed the tonic $GABA_AR$ current under whole-cell recording conditions within the slice (% suppression of tonic $GABA_AR$ current = 15.50 ± 2.27%, n = 20 cells from 6 animals), EtOH also significantly suppressed subsequent responses of isolated GCs to exogenous GABA, and to a similar degree (% suppression of GABA-induced current = 20.29 ± 7.76%, n = 6 cells from 2 animals; Fig. 7e,f). Upon washout of exogenous GABA, subsequent application of GABAzine did not generate any detectable currents (Fig. 7e), confirming that physically isolated GCs were not affected by endogenous GABA release from the slice. These results unequivocally demonstrate that EtOH can act directly on the

postsynaptic cell to suppress extrasynaptic $GABA_AR$ tonic current responses to a fixed concentration of GABA.

Low GC PKC activity enables postsynaptic EtOH action

Because tonic $GABA_AR$ currents in B6 and D2 mouse, and SDR GCs appear to be mediated by similar receptor subunits (α6βxδ; Fig. 1), but show a differential sensitivity to direct suppression by EtOH, we considered postsynaptic modulatory mechanisms that might alter $GABA_AR$ sensitivity to EtOH. Previous studies showed that genetic deletion of PKCγ reduced EtOH stimulation of $GABA_AR$-mediated Cl^- fluxes in a cerebellar microsac assay[31], but the microsac Cl^- flux assay does not provide any information about the cell types involved, the underlying type of $GABA_AR$ currents or the responsible $GABA_ARs$. In particular, with a mixed population of cells and $GABA_ARs$, it is possible that the reported global reduction of EtOH stimulation is achieved by increasing EtOH suppression of a subset of $GABA_ARs$, i.e. those mediating tonic $GABA_AR$ currents in GCs (PKCγ is heavily expressed in all cell layers of the cerebellum[32]). To test this possibility, we determined whether blocking PKC in SDR GCs converted their normally insensitive tonic $GABA_AR$ currents to being sensitive to EtOH-induced suppression (Fig. 8a,c). In the presence of TTX (to isolate direct suppressive actions of EtOH), addition of the PKC inhibitor, Calphostin C (100nM), to the recording electrode solution, transformed SDR GCs such that EtOH reduced the magnitude of the tonic $GABA_AR$ current (-1.03 ± 0.41 pA, n = 20 cells from 5 animals, P = .022) to a similar degree to what is observed in untreated B6 GCs (P = .47; Fig. 8a,c). Thus, insensitivity of SDR GC $GABA_AR$ tonic currents to direct suppression by EtOH is a consequence of ongoing postsynaptic PKC activity. We therefore tested whether activating postsynaptic PKC in B6 GCs prevents EtOH suppression of tonic $GABA_AR$ currents (Fig. 8b,c). As predicted, in recordings from B6 GCs (in TTX), including the phorbol esther PKC activator, PMA (100nM), in the recording electrode, abolished EtOH suppression of tonic $GABA_AR$ currents (0.02 ± 0.22, n = 8 cells from 2 animals, P = 0.94 by unpaired t-tests; Fig. 8b,c). The actions of PKC on $GABA_AR$ currents is specific to their sensitivity to EtOH, because neither inclusion of PMA in B6 GCs nor Calphostin C in SDR GCs affected the baseline magnitude of tonic $GABA_AR$ current (SDR control = 7.80 ± 1.42 pA; SDR Calphostin C = 7.75 ± 1.16 pA; B6 control = 10.97 ± 0.66 pA; B6 PMA = 8.30 ± 2.60 pA; all $P > 0.05$). Our data indicates that EtOH can directly suppress tonic $GABA_AR$ currents in all genotypes tested, but such direct suppression is prevented by elevated postsynaptic PKC activity, whether it occurs naturally, as in SDRs, or it is pharmacologically induced in rodent genotypes with lower basal PKC activity.

To determine the relative importance of PKC regulation of EtOH direct suppression versus nNOS regulation of EtOH enhancement (via increased GABA release), we repeated the PKC experiments in B6 mouse and SDR GCs under control conditions (i.e. without TTX; Fig. 8d). In recordings of SDR GCs with Calphostin C in the recording electrode, although EtOH still enhanced the tonic $GABA_AR$ current, the enhancement was significantly less than for control cells (Calphostin C = 1.81 ± 0.60 pA, n = 16 cells from 3 animals, P = .003; Fig. 8d). Conversely, in recordings of B6 GCs with PMA in the recording electrode, EtOH no longer suppressed the tonic $GABA_AR$ current, but rather slightly increased it (PMA = 0.67 ± 0.46 pA, n = 6 cells from 2 animals, P = .089 by Mann-Whitney U tests; Fig. 8d).

Combined with the nNOS experiments above, the data confirm that the net response to EtOH is determined by the balance between EtOH-induced increases in GABA release (via inhibition of nNOS) and direct suppression of postsynaptic $GABA_A$Rs, with genetic variations in the two processes determining net response phenotype.

Discussion

Genetic variation in response to EtOH

Genetic contribution to AUDs must, at some level, manifest as a differential response to EtOH, but little is known about the underlying neural substrates. Here we used patch-clamp recording in brain slices to directly assess differences in EtOH-related neural mechanisms across rodent genotypes with documented divergent EtOH related behaviors. We focused on the cerebellum because the severity of EtOH-induced disruption of cerebellar dependent behaviors is inversely related to risk for developing AUDs in humans[5,6] and excessive EtOH consumption in many rodent models[7-11]. We found that the impact of EtOH on GC $GABA_A$R transmission ranges from strong potentiation in high EtOH sensitivity/low EtOH consuming SDRs and D2s to strong suppression in low sensitivity/high consuming B6s, with intermediate impact in moderate sensitivity/moderate consuming WSR1 and WSP1 mice (Fig. 2i). While there are many factors that influence EtOH consumption by rodents, including taste[33,34], to our knowledge this is the first example of a cellular response to EtOH that varies in magnitude and polarity in parallel with EtOH behavioral phenotypes. And while it is unlikely that any one molecular process or brain region will fully explain a given EtOH phenotype, that a relationship between cellular response to EtOH and EtOH consumption (Fig. 2i) holds across species (rats and mice), across inbred mice strains (B6 and D2), and across selected lines of mice (WSR and WSP) suggests that there is some overlap in the genes that influence EtOH consumption and GC $GABA_A$R responses to EtOH. Importantly, in contrast to many brain regions (e.g. hippocampus, nucleus accumbens, thalamus, ventral tegmental area, substantia nigra)[35-39], where EtOH only affects $GABA_A$R transmission at concentrations far above those typically achieved during voluntary consumption by rodents or humans (≥ 50mM), both suppression and enhancement of GC $GABA_A$R transmission occur at low, readily achieved concentrations of alcohol (9-31mM; Fig. 2j,k). Thus, to the extent that EtOH actions at $GABA_A$Rs influence acute EtOH sensitivity or voluntary consumption levels[40,41], the distinctively high sensitivity GC $GABA_A$R transmission and clear variation in response magnitude and polarity across rodent genotypes (Fig. 2i) highlights such actions as a potential cellular substrate for genotypic differences in EtOH phenotypes. Future studies should test whether experimental manipulations of GC $GABA_A$R responses to EtOH influences EtOH sensitivity or consumption phenotype, and our identification of the molecular mediators of $GABA_A$R responses (discussed below) should provide necessary targets for such endeavors.

Our findings also have important implications for interpreting behavioral data from knockout and transgenic mice, which are often created on a B6 background. In particular, genetic deletion of the α6 or δ subunit in B6 mice, which eliminates GC tonic $GABA_A$R currents[15,18], does not affect EtOH-induced disruption of rotarod performance[42,43]. However, studies in low EtOH consuming CD-1 mice clearly indicate that the cerebellum is

the primary site of action for EtOH-induced disruption of performance on the rotarod[12], and, although controversial[21], studies in low drinking SDRs suggest that EtOH enhancement of tonic $GABA_AR$ inhibition in GCs is a primary mechanism of such disruption[20]. Our determination that EtOH has opposite actions on GC tonic $GABA_AR$ currents in B6 mice and SDRs may explain this apparent discrepancy. If the EtOH-induced suppression of tonic $GABA_AR$ currents observed in B6 mouse GCs is less disruptive of rotarod performance than the enhancement of tonic $GABA_AR$ currents observed in SDR GCs, then genetic deletions that eliminate tonic $GABA_AR$ currents in B6 mice would have less impact on EtOH disruption of rotarod performance than will manipulations of tonic $GABA_AR$ currents in SDR GCs. Importantly, B6 mice are less sensitive than D2 mice to EtOH disruption of rotarod performance[8], suggesting that indeed EtOH-induced suppression of $GABA_AR$ tonic currents in B6 mice is less disruptive of rotarod performance than potentiation of $GABA_AR$ tonic currents in D2 mice. Thus, accurate interpretations of past and future behavioral studies of EtOH in rodents with genetic or pharmacological alteration of α6 or δ subunits will require electrophysiological assessment of the actions of EtOH on GC tonic $GABA_AR$ currents specifically in the line or strain of rodent being tested. Here we provide this information for five frequently studied genotypes: B6 mice, D2 mice, WSR mice, WSP mice, and SDRs.

EtOH-induced enhancement of $GABA_AR$ transmission

In SDRs, EtOH-induced potentiation of GC $GABA_AR$ inhibition is mediated by an increase in action-potential dependent, vesicular GABA release from Golgi cells (Fig. 3a,b)[19-21]. The increase in vesicular GABA release causes an increase in the frequency of GC sIPSCs and the magnitude of the tonic $GABA_AR$ current, due to accumulation of GABA in the extrasynaptic space. It has been suggested that EtOH also binds directly to GC extrasynaptic $GABA_ARs$ and increases their affinity for GABA, the degree of which is influenced by a nucleotide polymorphism in the $GABA_AR$ α6 subunit[20]. Such a polymorphism could represent a mechanism for genetic control of GC $GABA_AR$ sensitivity to EtOH. However, in agreement with several other studies[19,21], in our hands, even at 79mM, EtOH did not cause detectable potentiation of GC tonic $GABA_AR$ currents in the presence of TTX (Fig. 3a,b), arguing against direct potentiation of extrasynaptic $GABA_ARs$ by EtOH. Furthermore, since under physiological conditions (no TTX), EtOH-induced increased vesicular GABA release is the predominant cause of EtOH-enhanced GC tonic $GABA_AR$ currents[19,21], genetic control over that process is likely to be a more powerful control point. Indeed, here we demonstrate that the EtOH-induced increase in vesicular GABA release is mediated by suppression of NOS, and that genetic variation in nNOS expression across rodent genotypes powerfully controls the degree to which EtOH potentiates GC $GABA_AR$ transmission. Strikingly, based on our analysis of immunocytochemistry and bioassay, we estimate that the expression level of nNOS in the granule cell layer of B6 mice is about 25% of the levels expressed in SDRs and D2 mice (Fig. 6). Correspondingly, less than 20% of B6 GCs exhibited EtOH potentiation of GC $GABA_AR$ tonic currents, compared to >90% of SDR GCs and ∼50% of D2 GCs (Fig. 2e). Our data do not address how blockade of nNOS leads to increased Golgi cell excitability, but recent studies suggest that suppression of the Na^+/K^+-ATPase and a K^+ conductance contribute to the EtOH–induced increase in Golgi cell firing[28], and both could be down-stream targets of NO. In particular, NO is known to

increase Na^+/K^+-ATPase activity[44], so EtOH induced suppression of nNOS could reduce Na^+/K^+-ATPase activity, with resultant depolarization of Golgi cells. Similarly, while the molecular identity of the K^+ conductance that contributes to increased Golgi cell excitability is unclear[28], many K^+ conductances are positively modulated by NO, either directly or indirectly via NO-induced cGMP production[45,46]. Thus, EtOH suppression of NOS could also contribute to the suppression of K^+ channels that increases Golgi cell firing.

EtOH-induced suppression of $GABA_AR$ transmission

It is widely accepted that enhancement of $GABA_AR$ transmission is a primary mechanism underlying the behavioral effects of EtOH[40,41]. Contrary to this prevailing thinking, here we report that EtOH suppresses tonic $GABA_AR$ currents in several rodent genotypes (Fig. 2). The suppression of tonic $GABA_AR$ is not accompanied by a decrease in the frequency of sIPSCs, and is not blocked by TTX, and is observed in physically isolated B6 GC responses to exogenous GABA, suggesting a direct action on the extrasynaptic $GABA_ARs$ that mediate tonic inhibition (Fig. 7). Recent studies of recombinantly expressed $GABA_ARs$ with various point mutations indicate that $GABA_AR$ subunits may have multiple counteracting sites of action for EtOH, with the net effect of EtOH being determined by the balance of inhibitory and enhancement sites[47-49]. However, to our knowledge, this is the first report of EtOH suppressing native $GABA_ARs$ *in situ*. Studies of cultured rat GCs indicated that EtOH suppressed $GABA_AR$ currents in some GCs but enhanced it in others, and the proportion of cells showing suppression was increased in cells that were recorded with the perforated-patch technique[50], suggesting that endogenous kinases or other endogenous $GABA_AR$ modulators determines the polarity of action of EtOH. Indeed, we determined that elevated postsynaptic PKC activity occludes EtOH suppression of tonic $GABA_AR$ currents, and that genetic differences in PKC activity determine whether EtOH suppression of GC tonic $GABA_AR$ currents occurs in a given rodent genotype (Fig. 8).

Interactions among EtOH targets determines net response

Taken together, our data demonstrate that there are two main mechanisms by which EtOH acts on GC $GABA_AR$ transmission: 1.) inhibition of nNOS which results in increased action-potential dependent vesicular release of GABA with a resultant increase in sIPSC frequency and tonic $GABA_AR$ current magnitude, and 2.) a direct inhibition of $\alpha_6\delta$-containing $GABA_ARs$ and the tonic $GABA_AR$ current they generate in cells with low PKC activity. Thus, genetic or pharmacological control over two distinct and opposing molecular actions of EtOH enables a fine tuning of GC tonic $GABA_AR$ responses along a spectrum from powerful enhancement to powerful suppression.

Methods

Preparation of brain slices

All procedures conform to the regulations detailed in the National Institutes of Health *Guide for the Care and Use of Laboratory Animals* and were approved by the Animal Care and Use Committee of the Oregon Health and Science University. Cerebellar slices were prepared acutely on each day of experimentation[14,17]. Male and female rodents (18-28 days old), randomized for each experiment, were housed between 2-6 animals/cage and

maintained on a standard light/dark cycle. Animals were anaesthetized with Isoflurane and killed by decapitation. The whole brain was rapidly isolated and immersed in ice cold (0-2°C) artificial cerebrospinal fluid (ACSF) containing (in mM): 124 NaCl, 26 $NaHCO_3$, 1 NaH_2PO_4, 2.5 KCl, 2.5 $CaCl_2$, 2 $MgCl_2$, 10 D-glucose, and bubbled with 95%O_2/5% CO_2 (pH 7.4). The cerebellum was dissected out of the brain and mounted, parallel to the sagittal plane, in a slicing chamber filled with ice cold (0-2°C) ACSF. Parasagittal slices (225μm) were made with a vibrating tissue slicer (Vibratome). Slices were incubated in warmed ACSF (33±1°C) for one hour after dissection and then held at 22-23°C until used. Kynurenic acid (1 mM) was included in the dissection, incubation and holding solution (to block glutamate receptors to reduce potential excitotoxic damage) but was omitted from the experimental solutions.

Electrophysiology

Slices were placed in a submersion chamber on an upright microscope, and viewed with an Olympus 60X (0.9 numerical aperture) water immersion objective with differential interference contrast and infrared optics. Slices were perfused with ACSF at a rate of ∼7ml/min at room temperature (22-24° C). Drugs were dissolved in ACSF and applied by bath perfusion. Visually identified granule cells were voltage-clamped (Vh = -60mV) with patch pipettes, constructed from thick-walled borosilicate glass capillaries and filled with an internal solution containing (in mM): CsCl 130, NaCl 4, $CaCl_2$ 0.5, HEPES 10, EGTA 5, MgATP 4, Na_2GTP 0.5, QX-314 5. Solutions were pH adjusted to 7.2-7.3 with CsOH. Electrode resistance was 4 to 10 MΩ. Cells were rejected if access resistance was greater than 15 MΩ, or if access resistance changed by > 15%, or if there were condition-independent changes in holding current. Note, the intracellular [Cl^-] sets E_{Cl}- to ∼0mV, which for the holding potentials used in all experiments (-60mV), results in $GABA_AR$ currents being inward (downward deflections in displays of the holding current). Accordingly enhancement and block/suppression of tonic $GABA_AR$-mediated currents are inward and outward respectively. In all cases, only one cell was recorded from a given slice. In cases where the slice was exposed to more than one drug or different doses of the same drug, the order of drug application was randomized across slices. In all cases of multiple drug exposures to the same slice, a stable baseline was obtained following washout of drug for a minimum of 4 minutes. However, control experiments were never done on slices that had been exposed to TTX, GABAzine, or incubated in L-NA as the efficacy and time required to adequately wash such drugs is preclusive of additional unrelated experimentation.

Immunocytochemistry

Slices were fixed in 4% paraformaldehyde in phosphate buffered saline (PBS) for 17 hours. Slices were then washed and incubated for 40 minutes in blocking solution (PBS, 0.5% Triton X-100, and bovine serum albumin [0.5mg/ml]). Next, they were incubated for 1-2 days with primary antibody in PBS and Triton. Slices were washed 3 times (10 minutes each) in PBS, then incubated for 45 minutes with an Alexa-conjugated secondary antibody. Slices were mounted in Citifluor and imaged with confocal microscopy. See reagents below for source and dilution of antibodies used.

DAF-FM detection of NO production

We used DAF-FM as a fluorescent biochemical assay of cellular NO production[51]. Slices were incubated in the relevant experimental condition (control, control + 52mM EtOH, or control + 300μM L-NA) for a 30 minute equilibration period, followed by addition of the DAF-FM (1μM) + the relevant experimental condition for 30 minutes, followed by washout of DAF-FM in the continued presence of the relevant experimental condition for 30 minutes. Following the exposure protocol, slices were fixed (as for immunocytochemistry, see above), and processed for confocal microscopy. Whole field emission analysis largely eliminates subjective bias, and so DAF-FM experiments were not performed blind to the conditions of the experiment.

Confocal microscopy

Images were acquired with a Zeiss confocal LSM780 laser scanning Microscope, using accompanying Zeiss software for acquisition, processing and subsequent analysis. A laser line falling within 20nm of the peak absorbance was used for each of the various fluorophores, with appropriate excitation, dichroic and emission filters. One of two objectives was used for all experiments: a 20×, 0.8 N.A. Plan Apochromat air objective (Fig. 4), or a 40×, 1.4 N.A. PlanApo oil-immersion objective (Figs. 1**&**6 and supplementary Figs. 3&4). Pinhole diameter and slice step thickness were optimized for the objective used. For $GABA_AR$ subunit distribution studies (Fig. 1), quantification of nNOS and GAD 65/67 expression (Fig. 6d&g), and quantification of NO sensitive fluorophore (DAF-AM) fluorescence emission (Fig. 4) stacks of image planes were acquired, and then projected into a single stacked image (10 μm thick). For a given fluorophore, digital gain and offset settings were identical for all images across all species and conditions. For quantification of GC encirclement by nNOS (Fig. 6a-d and Supplementary Fig. 3), a single image plane at 10μm from the surface of the slice was analyzed as follows. Individual GCs were identified by nuclear stain Hoechst 33342, and the nNOS signal was amplified until ∼5% of the pixels were saturated. Subsequently, an experimenter, blind to the experimental condition, analyzed individual GC nuclei for percent encirclement by detectable nNOS signal (as in Supplementary Fig. 3). Values were obtained from at least 3 animals of each species, at least 2 slices from each animal and at least 5 distinct regions of each slice.

Analysis of $GABA_AR$ currents

Membrane currents were acquired at 20 kHz, filtered at 10 kHz, and analyzed with pClamp (v.6.3) software (Axon Instruments, Foster City, CA). For analysis and display of sIPSCs, data were filtered at 2-5 kHz. The absolutely objective methodology used for analysis of $GABA_AR$ currents (automated measurement at fixed time points) obviated experimenter blinding, thus collection and analysis of all electrophysiological experiments were not performed blind to the experimental condition. When quantifying sIPSC occurrence, sIPSCs were defined as current deflections that have an amplitude (measured from the mean current) greater than the peak-to-peak amplitude of the current noise and with a decay time constant at least 3-fold slower than the rise time. The tonic current was assessed by fitting the Gaussian distribution of all data points not skewed by synaptic events from a point 3 pA to the left of the peak value to the rightmost (smallest) value of the histogram distribution

(see supplemental Fig. 1 for examples). Drug-induced changes in tonic $GABA_AR$ current magnitude and sIPSC frequency were calculated by comparing the amplitude/frequency in the drug versus the mean amplitude/frequency of the currents before and after drug application.

Statistics

All data are expressed as the mean ± the standard error of the mean. One-way ANOVA was used to detect significant main effects, and Student's t-tests were used for post hoc-analyses, while all other statistical comparisons were made with unpaired or one-sample t-tests. In all cases, statistical tests were two-tailed and we set the threshold for significance at $P < 0.05$. In some cases, parametric statistical techniques could not be used due to variable or antipodal responses that violated assumption of normally distributed data as determined by significant Shapiro-Wilk statistic ($P < .05$). In these cases (i.e. Figs. 2h, 3f, 6d,k&l, **and** 8d), we used non-parametric Kruskal-Wallis one-way analysis of variance tests with Dunn's method for pair wise comparison, or Mann-Whitney U tests where appropriate. In the figures, gray arrows point to an extended time scale of recording from different time points of the main trace. * signifies $P < 0.05$, ** signifies $P < 0.01$, and *** signifies $P < 0.001$. No statistical methods were used to pre-determine sample sizes but our sample sizes are similar to those reported in the field[14,17,19,20].

Reagents

All reagents were from Sigma Chemicals (St. Louis, MO) except AP5, bicuculline, gabazine, kynurenic acid, NBQX (all from Ascent scientific, UK), and iodoacetic acid (from Acros/Fisher). Primary antibodies were (host/supplier/dilution): nNOS (rabbit/Cayman chemicals 160870/1:200), GAD65 (mouse/Millipore MAB 351/1:200), GAD67 (mouse/Millipore MAP 5406/1:200), α6 subunit of $GABA_AR$ (rabbit/Millipore AB5610/1:200) δ subunit of $GABA_AR$ (rabbit/Millipore AB9752/1:200). Secondary antibodies were various excitation maxima Alexafluors (Invitrogen) from appropriate hosts diluted 1:500. For some antibodies (α6 and δ subunit of $GABA_AR$), specificity has been confirmed by lack of labeling in relevant knockout mice, for others (GAD 65 and 67) specificity has been confirmed by their labeling of a single band on western blots (see manufacturer website for details, and links therein). For those antibodies where such confirmation of specificity was not already available (nNOS), we confirmed specificity ourselves, by examining slices from nNOS knockout mice (*Nos1*^{tm1Plh} homozygotes, backcrossed to C57BL/6J mice for >10 generations, from Jackson Laboratory), which did not display detectable nNOS staining (Supplementary Fig. 4). Furthermore, for all of the antibodies we used, the general qualitative expression pattern within the cerebellum is similar to what has been shown with other antibodies in other reports and to our own studies with alternative antibodies. Importantly, for all of the crucial immunohistochemical studies ($GABA_AR$ subunits and nNOS), we have conducted parallel electrophysiological studies of the relevant proteins' activity which confirm our histochemical assessments (see electrophysiological experiments in Figs. 1**&**6 for functional confirmation of $GABA_AR$ subunit and NOS expression levels, respectively).

Supplementary Material

Refer to Web version on PubMed Central for supplementary material.

Acknowledgments

We thank Drs. John Crabbe, Deb Finn and Kris Wiren (Oregon Health & Science University) for discussions about the research, and Dr. David Atwell (University College London) for comments on the manuscript. This study was supported by National Institute of Neurological Disorders and Stroke Grant R01NS051561, National Institute on Alcohol Abuse and Alcoholism Grant R01AA012439, American Heart Association Grant in Aid, and Medical Research Foundation of Oregon grant to D.J.R., training grants T32 AA007468 and F31 AA022267 from the National Institute on Alcohol Abuse and Alcoholism, and an OHSU Research Scholars Award for J.S.K., and the Neuroscience Imaging Center at OHSU grant P30NS061800 from the National Institute of Neurological Disorders and Stroke.

References

1. Harwood, H. National Institute on Alcohol Abuse and Alcoholism; 2000. Updating Estimates of the Economic Costs of Alcohol Abuse in the United States: Estimates, Update Methods, and Data. http://pubs.niaaa.nih.gov/publications/economic-2000/
2. Hill SY. Neural plasticity, human genetics, and risk for alcohol dependence. Int Rev Neurobiol. 2010; 91:53–94. [PubMed: 20813240]
3. Prescott CA, Kendler KS. Genetic and environmental contributions to alcohol abuse and dependence in a population-based sample of male twins. Am J Psychiatry. 1999; 156:34–40. [PubMed: 9892295]
4. Herting MM, Fair D, Nagel BJ. Altered fronto-cerebellar connectivity in alcohol-naive youth with a family history of alcoholism. Neuroimage. 2011; 54:2582–2589. [PubMed: 20970506]
5. Schuckit MA, Tsuang JW, Anthenelli RM, Tipp JE, Nurnberger JI Jr. Alcohol challenges in young men from alcoholic pedigrees and control families: a report from the COGA project. J Stud Alcohol. 1996; 57:368–377. [PubMed: 8776678]
6. Schuckit MA, Smith TL, Kalmijn J, Danko GP. A cross-generational comparison of alcohol challenges at about age 20 in 40 father-offspring pairs. Alcohol Clin Exp Res. 2005; 29:1921–1927. [PubMed: 16340447]
7. Yoneyama N, Crabbe JC, Ford MM, Murillo A, Finn DA. Voluntary ethanol consumption in 22 inbred mouse strains. Alcohol. 2008; 42:149–160. [PubMed: 18358676]
8. Gallaher EJ, Jones GE, Belknap JK, Crabbe JC. Identification of genetic markers for initial sensitivity and rapid tolerance to ethanol-induced ataxia using quantitative trait locus analysis in BXD recombinant inbred mice. J Pharmacol Exp Ther. 1996; 277:604–612. [PubMed: 8627537]
9. Bell RL, Stewart RB, Woods JE, Lumeng L, Li TK, Murphy JM, McBride WJ. Responsivity and development of tolerance to the motor impairing effects of moderate doses of ethanol in alcohol-preferring (P) and -nonpreferring (NP) rat lines. Alcohol Clin Exp Res. 2001; 25:644–650. [PubMed: 11371712]
10. Malila A. Intoxicating effects of three aliphatic alcohols and barbital on two rat strains genetically selected for their ethanol intake. Pharmacol Biochem Behav. 1978; 8:197–201. [PubMed: 652828]
11. McClearn, GE.; Deitrich, RA.; Erwin, VG. National Institute of Alcohol Abuse and Alcoholism Research Monograph. Washington DC: 1981. Development of Animal Models as Pharmacogentic Tools.
12. Al Rejaie S, Dar MS. Antagonism of ethanol ataxia by intracerebellar nicotine: possible modulation by mouse cerebellar nitric oxide and cGMP. Brain Res Bull. 2006; 69:187–196. [PubMed: 16533669]
13. Duguid I, Branco T, London M, Chadderton P, Hausser M. Tonic inhibition enhances fidelity of sensory information transmission in the cerebellar cortex. J Neurosci. 2012; 32:11132–11143. [PubMed: 22875944]
14. Hamann M, Rossi DJ, Attwell D. Tonic and spillover inhibition of granule cells control information flow through cerebellar cortex. Neuron. 2002; 33:625–633. [PubMed: 11856535]

15. Brickley SG, Revilla V, Cull-Candy SG, Wisden W, Farrant M. Adaptive regulation of neuronal excitability by a voltage-independent potassium conductance. Nature. 2001; 409:88–92. [PubMed: 11343119]
16. Meera P, Wallner M, Otis TS. Molecular basis for the high THIP/gaboxadol sensitivity of extrasynaptic GABAA receptors. J Neurophysiol. 2011
17. Rossi DJ, Hamann M, Attwell D. Multiple modes of GABAergic inhibition of rat cerebellar granule cells. J Physiol. 2003; 548:97–110. [PubMed: 12588900]
18. Stell BM, Brickley SG, Tang CY, Farrant M, Mody I. Neuroactive steroids reduce neuronal excitability by selectively enhancing tonic inhibition mediated by delta subunit-containing GABAA receptors. Proc Natl Acad Sci U S A. 2003; 100:14439–14444. [PubMed: 14623958]
19. Carta M, Mameli M, Valenzuela CF. Alcohol enhances GABAergic transmission to cerebellar granule cells via an increase in Golgi cell excitability. J Neurosci. 2004; 24:3746–3751. [PubMed: 15084654]
20. Hanchar HJ, Dodson PD, Olsen RW, Otis TS, Wallner M. Alcohol-induced motor impairment caused by increased extrasynaptic GABA(A) receptor activity. Nat Neurosci. 2005; 8:339–345. [PubMed: 15696164]
21. Botta P, Radcliffe RA, Carta M, Mameli M, Daly E, Floyd KL, Deitrich RA, Valenzuela CF. Modulation of GABAA receptors in cerebellar granule neurons by ethanol: a review of genetic and electrophysiological studies. Alcohol. 2007; 41:187–199. [PubMed: 17521847]
22. Melchior CL, Myers RD. Genetic differences in ethanol drinking of the rat following injection of 6-OHDA, 5,6-DHT or 5,7-DHT into the cerebral ventricles. Pharmacol Biochem Behav. 1976; 5:63–72. [PubMed: 996042]
23. Korpi ER, Kuner T, Seeburg PH, Luddens H. Selective antagonist for the cerebellar granule cell-specific gamma-aminobutyric acid type A receptor. Mol Pharmacol. 1995; 47:283–289. [PubMed: 7870036]
24. Saxena NC, Macdonald RL. Properties of putative cerebellar gamma-aminobutyric acid A receptor isoforms. Mol Pharmacol. 1996; 49:567–579. [PubMed: 8643098]
25. De Schutter E, Bower JM. An active membrane model of the cerebellar Purkinje cell II. Simulation of synaptic responses. J Neurophysiol. 1994; 71:401–419. [PubMed: 8158238]
26. Ford MM, Fretwell AM, Anacker AM, Crabbe JC, Mark GP, Finn DA. The influence of selection for ethanol withdrawal severity on traits associated with ethanol self-administration and reinforcement. Alcohol Clin Exp Res. 2011; 35:326–337. [PubMed: 21070250]
27. Porcu P, O'Buckley TK, Alward SE, Song SC, Grant KA, de Wit H, Leslie MA. Differential effects of ethanol on serum GABAergic 3alpha,5alpha/3alpha,5beta neuroactive steroids in mice, rats, cynomolgus monkeys, and humans. Alcohol Clin Exp Res. 2010; 34:432–442. [PubMed: 20028362]
28. Botta P, Simoes de Souza FM, Sangrey T, De Schutter E, Valenzuela CF. Excitation of Rat Cerebellar Golgi Cells by Ethanol: Further Characterization of the Mechanism. Alcohol Clin Exp Res. 2011
29. Fataccioli V, Gentil M, Nordmann R, Rouach H. Inactivation of cerebellar nitric oxide synthase by ethanol in vitro. Alcohol Alcohol. 1997; 32:683–691. [PubMed: 9463722]
30. Wall MJ. Endogenous nitric oxide modulates GABAergic transmission to granule cells in adult rat cerebellum. Eur J Neurosci. 2003; 18:869–878. [PubMed: 12925012]
31. Harris RA, McQuilkin SJ, Paylor R, Abeliovich A, Tonegawa S, Wehner JM. Mutant mice lacking the gamma isoform of protein kinase C show decreased behavioral actions of ethanol and altered function of gamma-aminobutyrate type A receptors. Proc Natl Acad Sci U S A. 1995; 92:3658–3662. [PubMed: 7731960]
32. Naik MU, Benedikz E, Hernandez I, Libien J, Hrabe J, Valsamis M, Dow-Edwards D, Osman M, Sacktor TC. Distribution of protein kinase Mzeta and the complete protein kinase C isoform family in rat brain. J Comp Neurol. 2000; 426:243–258. [PubMed: 10982466]
33. Fidler TL, Dion AM, Powers MS, Ramirez JJ, Mulgrew JA, Smitasin PJ, Crane AT, Cunningham CL. Intragastric self-infusion of ethanol in high- and low-drinking mouse genotypes after passive ethanol exposure. Genes Brain Behav. 2011; 10:264–275. [PubMed: 21091635]

34. McCool BA, Chappell AM. Using monosodium glutamate to initiate ethanol self-administration in inbred mouse strains. Addict Biol. 2012; 17:121–131. [PubMed: 21054690]
35. Jia F, Chandra D, Homanics GE, Harrison NL. Ethanol modulates synaptic and extrasynaptic GABAA receptors in the thalamus. J Pharmacol Exp Ther. 2008; 326:475–482. [PubMed: 18477766]
36. Liang J, Zhang N, Cagetti E, Houser CR, Olsen RW, Spigelman I. Chronic intermittent ethanol-induced switch of ethanol actions from extrasynaptic to synaptic hippocampal GABAA receptors. J Neurosci. 2006; 26:1749–1758. [PubMed: 16467523]
37. Nie Z, Madamba SG, Siggins GR. Ethanol enhances gamma-aminobutyric acid responses in a subpopulation of nucleus accumbens neurons: role of metabotropic glutamate receptors. J Pharmacol Exp Ther. 2000; 293:654–661. [PubMed: 10773041]
38. Peris J, Coleman-Hardee M, Burry J, Pecins-Thompson M. Selective changes in GABAergic transmission in substantia nigra and superior colliculus caused by ethanol and ethanol withdrawal. Alcohol Clin Exp Res. 1992; 16:311–319. [PubMed: 1317135]
39. Theile JW, Morikawa H, Gonzales RA, Morrisett RA. Role of 5-hydroxytryptamine2C receptors in Ca2+-dependent ethanol potentiation of GABA release onto ventral tegmental area dopamine neurons. J Pharmacol Exp Ther. 2009; 329:625–633. [PubMed: 19225162]
40. Criswell HE, Ming Z, Kelm MK, Breese GR. Brain regional differences in the effect of ethanol on GABA release from presynaptic terminals. J Pharmacol Exp Ther. 2008; 326:596–603. [PubMed: 18502983]
41. Kumar S, Porcu P, Werner DF, Matthews DB, Diaz-Granados JL, Helfand RS, Morrow AL. The role of GABA(A) receptors in the acute and chronic effects of ethanol: a decade of progress. Psychopharmacology (Berl). 2009; 205:529–564. [PubMed: 19455309]
42. Korpi ER, Koikkalainen P, Vekovischeva OY, Makela R, Kleinz R, Uusi-Oukari M, Wisden W. Cerebellar granule-cell-specific GABAA receptors attenuate benzodiazepine-induced ataxia: evidence from alpha 6-subunit-deficient mice. Eur J Neurosci. 1999; 11:233–240. [PubMed: 9987027]
43. Mihalek RM, Bowers BJ, Wehner JM, Kralic JE, VanDoren MJ, Morrow AL, Homanics GE. GABA(A)-receptor delta subunit knockout mice have multiple defects in behavioral responses to ethanol. Alcohol Clin Exp Res. 2001; 25:1708–1718. [PubMed: 11781502]
44. White CN, Hamilton EJ, Garcia A, Wang D, Chia KK, Figtree GA, Rasmussen HH. Opposing effects of coupled and uncoupled NOS activity on the Na+-K+ pump in cardiac myocytes. Am J Physiol Cell Physiol. 2008; 294:C572–C578. [PubMed: 18057120]
45. Salapatek AM, Wang YF, Mao YK, Mori M, Daniel EE. Myogenic NOS in canine lower esophageal sphincter: enzyme activation, substrate recycling, and product actions. Am J Physiol. 1998; 274:C1145–C1157. [PubMed: 9575812]
46. Wang W, Hebert SC, Giebisch G. Renal K+ channels: structure and function. Annu Rev Physiol. 1997; 59:413–436. [PubMed: 9074771]
47. Johnson WD, Howard RJ, Trudell JR, Harris RA. The TM2 6′ position of GABA(A) receptors mediates alcohol inhibition. J Pharmacol Exp Ther. 2012; 340:445–456. [PubMed: 22072732]
48. Mihic SJ, Ye Q, Wick MJ, Koltchine VV, Krasowski MD, Finn SE, Mascia MP, Valenzuela CF, Hanson KK, Greenblatt EP, Harris RA, Harrison NL. Sites of alcohol and volatile anaesthetic action on GABA(A) and glycine receptors. Nature. 1997; 389:385–389. [PubMed: 9311780]
49. Ueno S, Lin A, Nikolaeva N, Trudell JR, Mihic SJ, Harris RA, Harrison NL. Tryptophan scanning mutagenesis in TM2 of the GABA(A) receptor alpha subunit: effects on channel gating and regulation by ethanol. Br J Pharmacol. 2000; 131:296–302. [PubMed: 10991923]
50. Yamashita M, Marszalec W, Yeh JZ, Narahashi T. Effects of ethanol on tonic GABA currents in cerebellar granule cells and mammalian cells recombinantly expressing GABA(A) receptors. J Pharmacol Exp Ther. 2006; 319:431–438. [PubMed: 16844844]
51. Kojima H, Nakatsubo N, Kikuchi K, Kawahara S, Kirino Y, Nagoshi H, Hirata Y, Nagano T. Detection and imaging of nitric oxide with novel fluorescent indicators: diaminofluoresceins. Anal Chem. 1998; 70:2446–2453. [PubMed: 9666719]

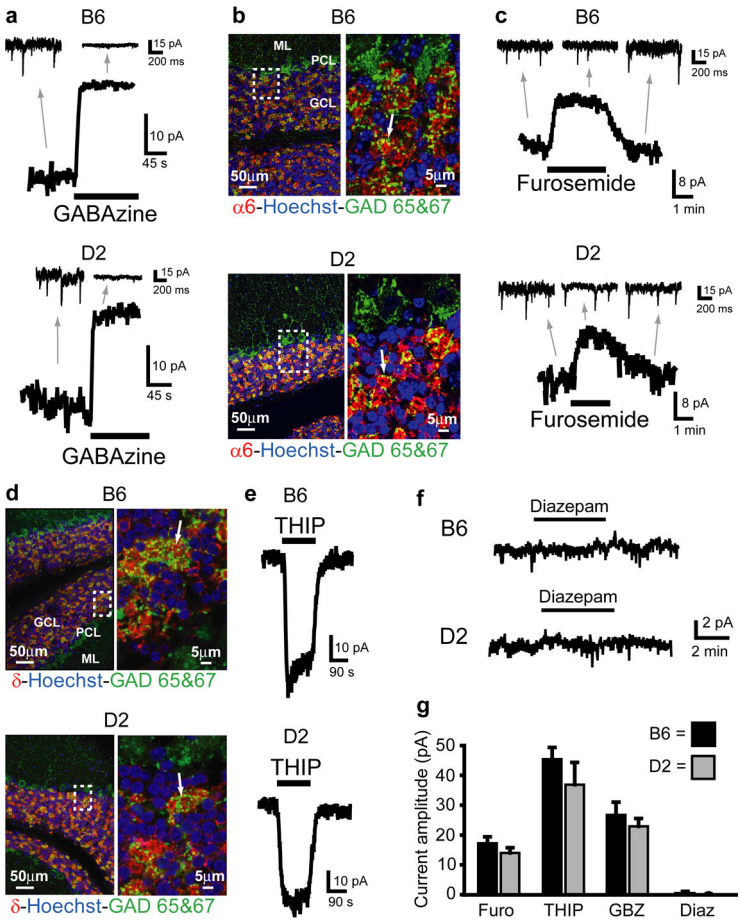

Figure 1.

B6 and D2 mouse GCs exhibit similar magnitude tonic currents mediated by α6 and δ subunit containing $GABA_A$Rs. **a.** Example traces showing block of tonic current by $GABA_A$R antagonist GABAzine (10µM) in GCs from B6 (**top**) and D2 (**bottom**) mice. Note, in this and all other figures, the gray arrows point to an expanded time scale of recording from different time points of the main traces (coming from the region of the main trace that the back of the arrow extrapolates to), showing sIPSCs and block by GABAzine. **b.** Confocally acquired fluorescence images of cerebellar slices from B6 (**top**) and D2 (**bottom**) mice (representative scans from n = 8 slices from 4 B6s and n = 7 slices from 4 D2s) showing α6 subunit of the $GABA_A$R (red) expression exclusively in the granule cell layer (identified by high density of GC nuclei, labeled blue with nuclear stain Hoechst, beneath the Purkinje cell layer, labeled green with antibody to GAD, left panels). Right panels are blow ups of boxed region showing α6 staining is around GC somas (labeled blue with nuclear stain Hoechst), and in GC dendrites located in the glomerulus (indicated by lack of nuclear stain, and colocalization with staining for GAD (green) which labels Golgi cell axon terminals). Arrow points to a representative α6 labeled glomerulus. GCL=GC layer, PCL=Purkinje cell layer, ML=Molecular layer. **c.** Example traces showing block of tonic current by $GABA_A$R antagonist furosemide (100µM, at which concentration it is

specific for $GABA_AR$s containing the α6 subunit) in GCs from B6 (**top**) and D2 (**bottom**) mice. Gray arrows point to expanded time scale of recording from different time points of main traces, showing lack of effect of furosemide on sIPSCs. **d.** Same as C&D except red immunostain comes from antibody for the δ subunit of the $GABA_AR$ (representative scans from $n = 5$ slices from 4 B6s and $n = 9$ slices from 6 D2s). **e.** Example traces showing enhancement of tonic current by $GABA_AR$ agonist THIP (500nM, at which concentration it is specific for $GABA_AR$s containing the δ subunit) in GCs from B6 (**top**) and D2 (**bottom**) mice. **f.** Example traces showing lack of effect of diazepam (300nM) on tonic $GABA_AR$ current in GCs from B6 (top) and D2 (bottom) mice. **g.** Plot summarizing mean tonic current induced by THIP (B6, $n = 18$ cells; D2, $n = 10$), and blocked by furosemide (B6, $n = 17$ cells; D2, $n = 17$) and GABAzine (B6, $n = 12$ cells; D2, $n = 12$), and lack of effect of diazepam (B6, n = 7 cells; D2, n = 9) in B6 and D2 mouse GCs. Furosemide-, THIP- and GABAzine-, but not diazepam-induced currents ($n = 16$ cells, $P = .49$), are all significantly different from zero $P < 0.05$ using one-sample *t*-tests, and none are significantly different between strains (furosemide: $P = .25$; THIP: $P = .27$; GABAzine: $P = .45$, unpaired *t*-tests).

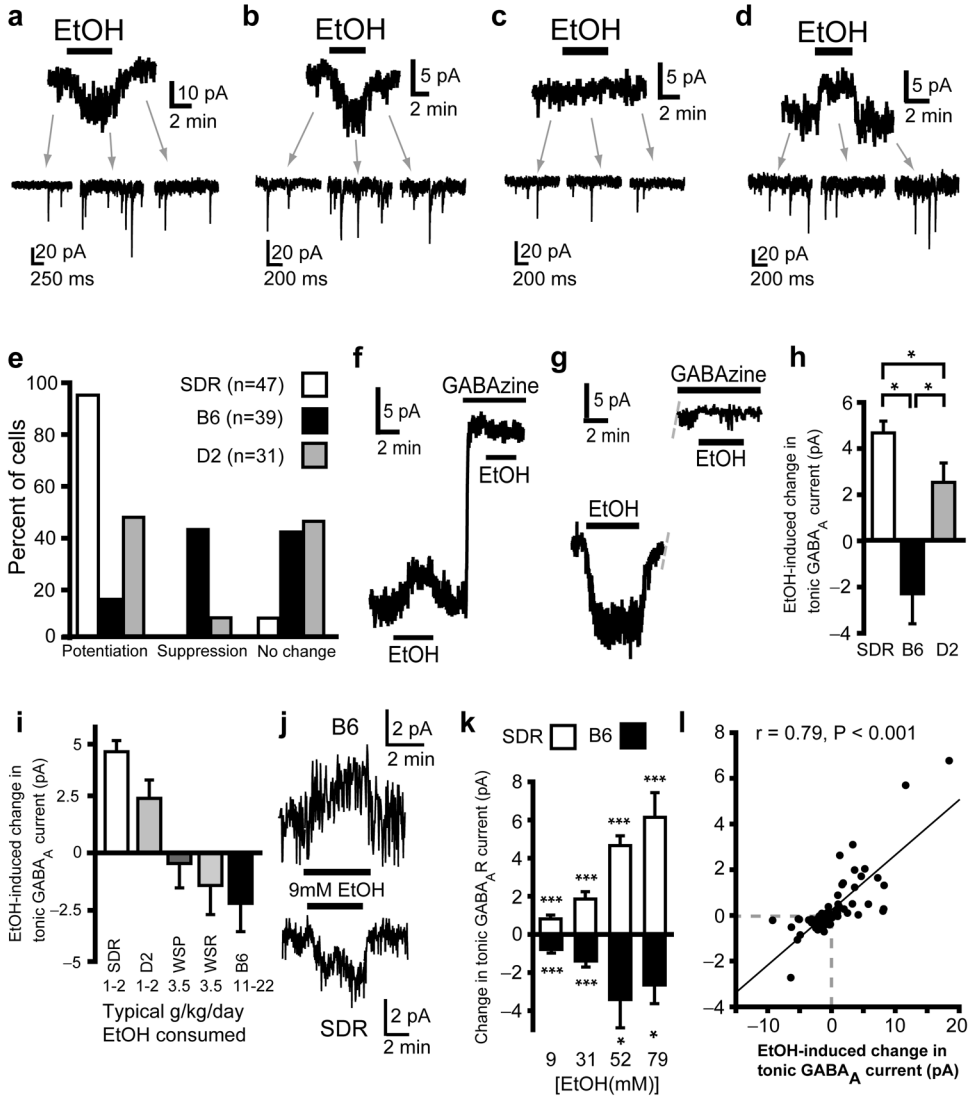

Figure 2.

The impact of EtOH on GC tonic $GABA_AR$ currents varies in polarity and magnitude across rodent genotypes with divergent EtOH consumption phenotypes. **a.** Representative data showing that EtOH increases sIPSC frequency (insets indicated by gray arrows) and potentiates the tonic $GABA_AR$ current magnitude (main trace) in SDR GCs. **b-d.** Representative data showing that EtOH can either potentiate (**b**), suppress (**d**) or have no impact (**c**) on tonic $GABA_AR$ currents in D2 and B6 GCs. **e.** Plot of proportion of GCs showing potentiation, suppression or no effect of EtOH on tonic $GABA_AR$ currents in SDR, B6 and D2 GCs. **f&g.** Representative traces showing that both outward (**f**) and inward (**g**) currents induced by EtOH are abolished by the $GABA_AR$ antagonist, GABAzine (10μM). For cells that had shown significant EtOH-induced inward and outward currents under control conditions, in the presence of GABAzine, the mean EtOH-induced current was -0.09 ± 0.16 pA and -0.13 ± 0.22 pA, i.e. not significantly different to baseline for both (Inward: *n*

= 13 cells, $P = .55$; outward: $n = 14$, $P = 0.53$, one-sample *t*-tests). **h.** Plot of the mean magnitude and polarity of the GC $GABA_A$ tonic current to EtOH for all cells tested from SDRs, B6s and D2s (* indicates significantly different, $P < 0.05$). **i.** Plot of the mean magnitude and polarity of the GC $GABA_A$ tonic current to EtOH for all cells from each type of rodent: SDRs ($n = 47$ cells), D2 mice ($n = 31$), WSP mice ($n = 9$), WSR mice ($n = 7$), and B6 mice ($n = 39$). Numbers at bottom of chart show the typical amount of EtOH consumed (in g/kg/day) for each type of rodent in published free access two or three bottle choice studies (from[7,22,26]). **j.** Representative traces showing that concentrations of EtOH as low as 9mM suppress and enhance tonic $GABA_A$R currents in B6 mouse and SD rat GCs respectively. **k.** Plot showing dose response relationship for EtOH-induced suppression and enhancement of tonic $GABA_A$R current from baseline in B6 mouse (black) and SD rat (white) GCs respectively (SD rat: all ***$P < .001$; B6: ***$P < .001$ [9mM], ***$P < .001$ [31mM], *$P = .028$ [52mM]; $P = .025$ [79mM], one-sample *t*-tests). **l.** Plot of EtOH induced change in tonic $GABA_A$R current magnitude versus EtOH-induced change in noise variance for each cell examined (all concentrations of EtOH tested 9-79 mM are included; SD rat: $n = 16$ cells; B6: $n = 27$; D2: $n = 36$).

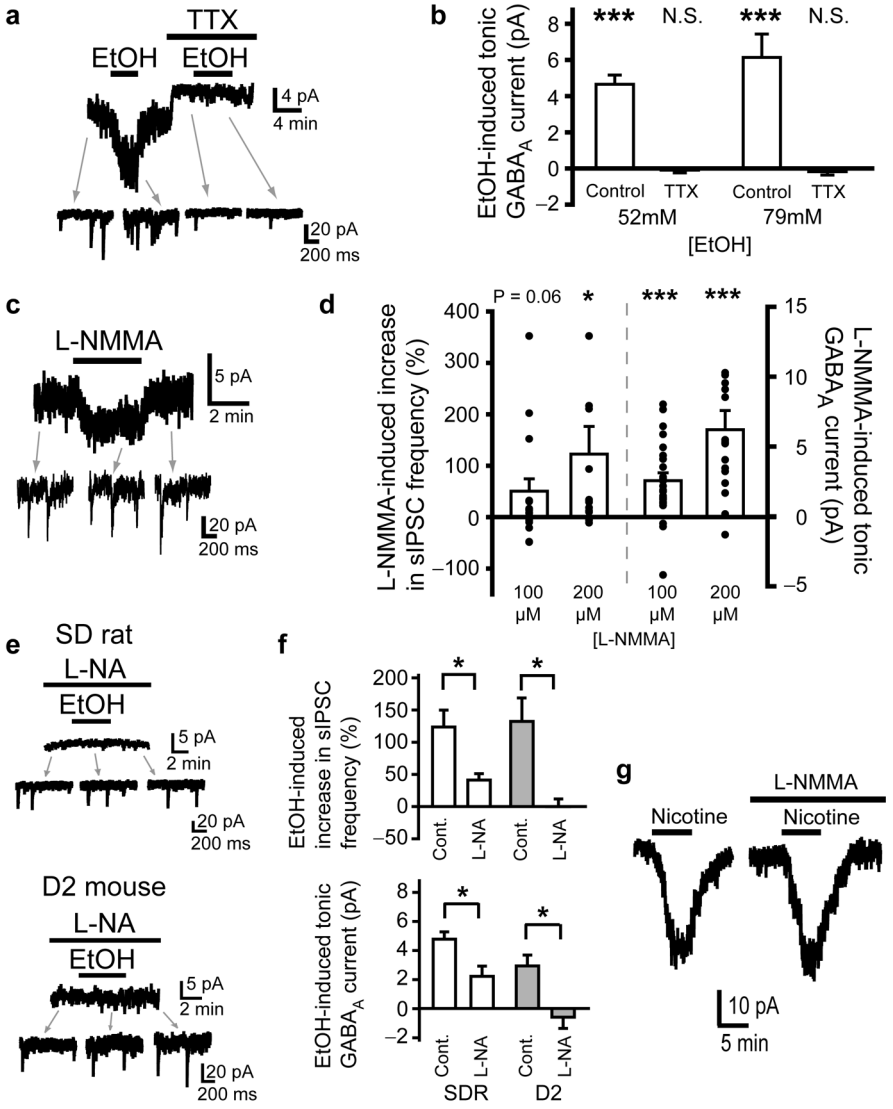

Figure 3.

EtOH-induced potentiation of GC tonic GABA$_A$R current is mediated by suppression of NOS and consequent increase in action potential dependent vesicular release of GABA. **a.** Representative recording shows that blocking action potentials with TTX (500nM) abolishes the EtOH (52mM)-induced increase in sIPSCs and tonic GABA$_A$R current magnitude. **b.** Chart depicts mean magnitude of EtOH-induced (52mM and 79mM) increase in tonic GABA$_A$R current under control conditions (n = 47 cells for 52mM; n = 15 for 79mM) and in the presence of TTX (500nM; n = 11 cells from 3 animals for 52mM; n = 8 cells from 2 animals for 79mM). EtOH effects in TTX did not significantly differ from baseline, P = .54 for 52mM EtOH and P = .36 for 79mM EtOH; *** indicates significantly different from baseline $P < 0.001$ by one-sample t-tests. **c.** Representative recording shows that the NOS substrate inhibitor, L-NMMA (100µM) increases the frequency of sIPSCs and the tonic GABA$_A$R current in SDR GCs. L-NMMA had no effect on GC currents in the presence of

the $GABA_AR$ antagonist, GABAzine (10μM, *n* = 4 cells from 2 animals, not shown). **d.** Plot of mean increase in sIPSC frequency (left; 100uM: *n* = 22 cells from 10 animals, 48.34 ± 23.97%, *P* = .057; 200uM: *n* = 16 cells from 5 animals, 120.37 ± 53.94%, **P* = .044, by one-sample *t*-tests) and tonic $GABA_AR$ current magnitude (right; 100uM: *n* = 22 cells, 2.56 ± 0.56, ****P* < .001; 200uM: *n* = 16, 6.20 ± 1.38, ****P* < .001, by one-sample *t*-tests) induced by L-NMMA in SDR GCs. **e.** Representative recordings showing that pre-incubation of slices and maintained presence in the NOS substrate inhibitor, L-NA (300μM), suppresses the EtOH-induced increase in sIPSCs and tonic $GABA_AR$ current in SDR (**top**) and D2 (**bottom**) GCs. **f.** Plots of mean increase in sIPSC frequency (**top**) and tonic $GABA_AR$ current magnitude (**bottom**) induced by EtOH (52mM) in SDR (white; *n* = 10 cells from 3 animals for L-NA treated slices, sIPSCs: **P* = .015; tonic $GABA_AR$ current: **P* = .026) and D2 (gray; *n* = 8 cells from 2 animals for L-NA treated slices, sIPSCs: **P* = .015; tonic $GABA_AR$ current: **P* = .029, comparisons between groups by Mann-Whitney U tests) GCs under control conditions and in slices treated with L-NA (300μM). **g.** Representative traces showing that the NOS antagonist, L-NMMA (200μM) does not block nicotine (500nM)-induced increases in tonic $GABA_AR$ currents in SDR GCs. **M**ean increase in tonic $GABA_AR$ current magnitude induced by nicotine (500nM) in SDR GCs under control conditions = 17.56 ± 3.24 pA and in slices treated with L-NMMA (200μM) = 21.36 ± 5.61 pA (*n* = 5 cells from 2 animals, *P* = 0.46, paired *t*-test).

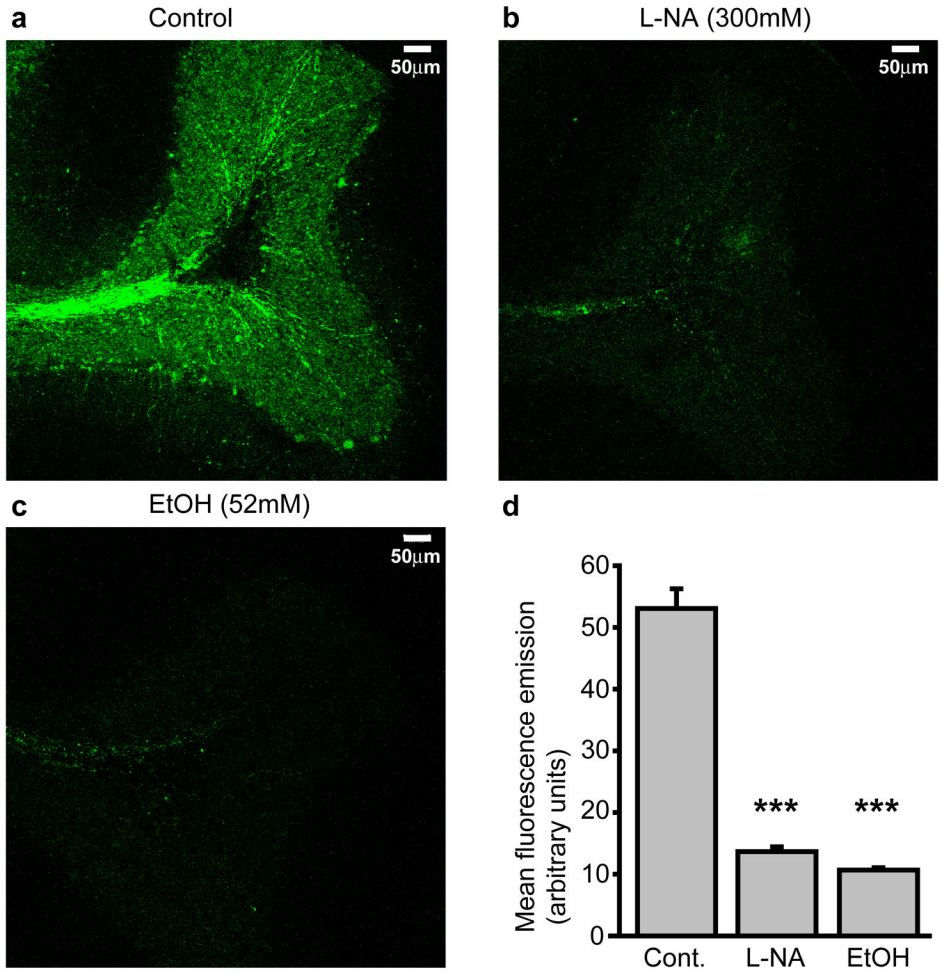

Figure 4.

EtOH suppresses tonic production of NO in the granule cell layer. **a-c**. Confocally acquired images of fluorescence emission from SDR cerebellar slices that were pre-soaked in either the NO-sensitive fluorophore, DAF-FM alone (**a**), or combined with the NOS antagonist, L-NA (300μM; **b**) or EtOH (52mM; **c**). **d.** Plot of mean DAF fluorescence emission across the granule cell layer under control conditions (n = 20 slices from 2 animals), or when treated with L-NA (300μM, n = 22 slices from 2 animals) or EtOH (52mM, n = 20 slices from 2 animals). *** indicates significantly different from control slices, $P < 0.001$, unpaired t-tests.

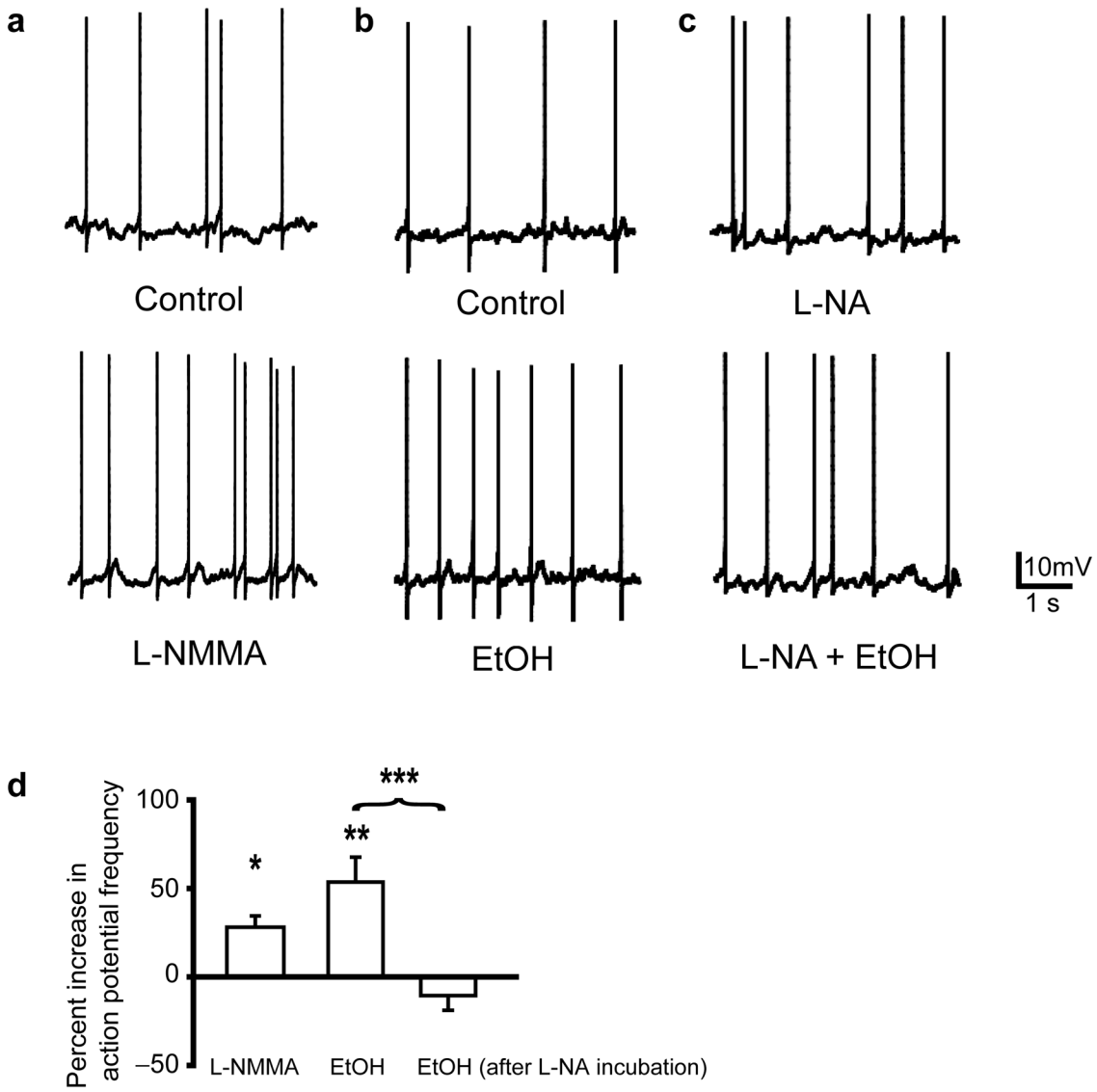

Figure 5.

EtOH inhibition of NOS increases Golgi cell firing. **a-c.** Representative traces show action potentials (APs) in current-clamped Golgi cells under various conditions: **a.** Control (**top**) versus the NOS antagonist, L-NMMA (200μM, **bottom**) in the same cell, **b.** control (**top**) versus EtOH (52mM, **bottom**) in the same cell, and **c.** in the presence of the NOS antagonist, L-NA (300μM, top) alone or with EtOH (52mM, bottom) in the same cell. **d.** Plot of mean increase in Golgi cell AP firing frequency in L-NMMA (200μM; $n = 4$ cells, $*P = .022$, one-sample t-test), EtOH (52μM; $n = 9$, $**P = .007$), or EtOH after incubation and in the presence of the NOS antagonist, L-NA (300μM, $n = 9$, $P = .24$, one-sample t-tests). Unpaired t-test comparing conditions, $**P = .001$.

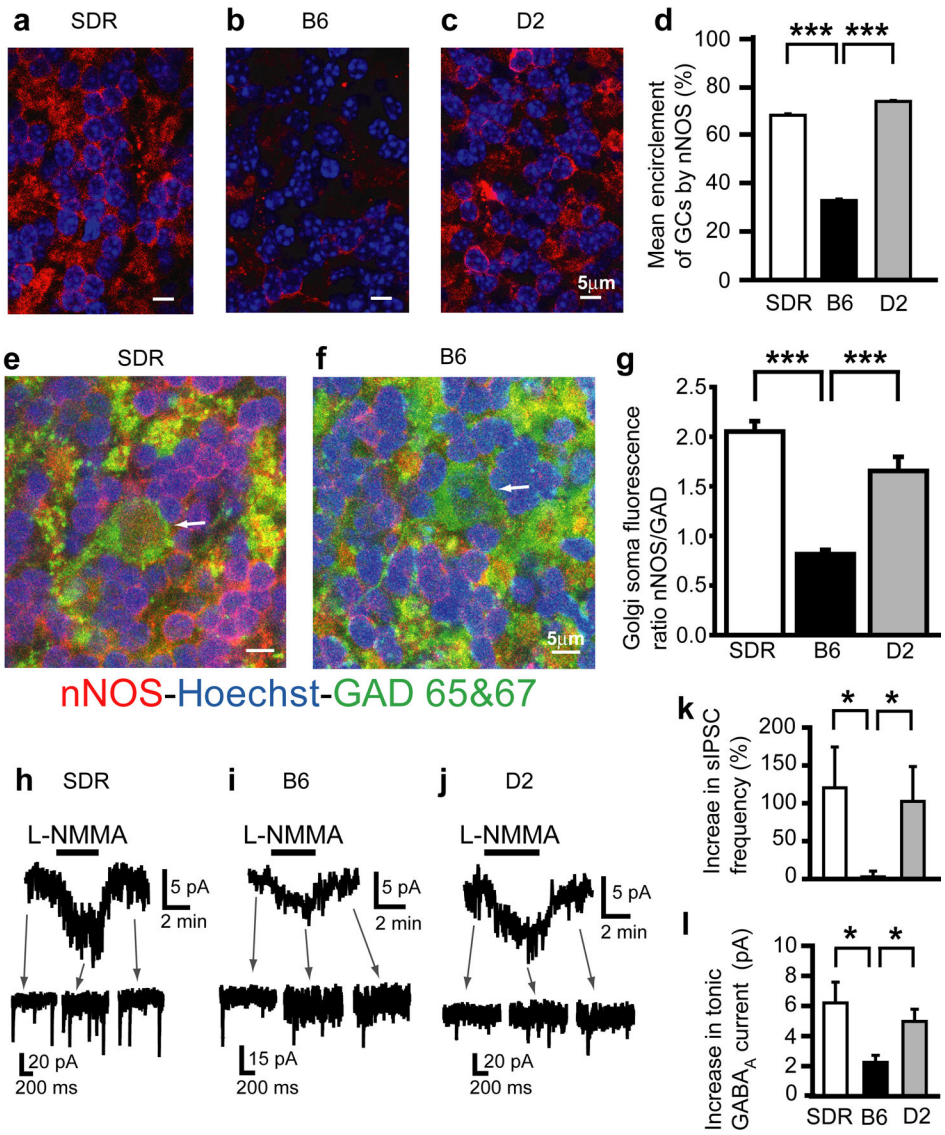

Figure 6.

Differential expression of nNOS underlies differences in EtOH-induced potentiation of GC $GABA_AR$ transmission. **a-c.** Confocally acquired images of immunocytochemistry for nNOS (red) and nuclear stain Hoechst (blue) in the granule cell layer of SDR (**a**), B6 (**b**), and D2 (**c**) cerebellum. **d.** Plot of mean percent encirclement of GC soma/nuclei (as determined in Supplementary Fig. 1) for SDR (white; n = 2694 cells from 2 slices from 2 animals), B6 (black; n = 2316 cells from 6 slices from 2 animals) and D2 (gray; n = 3398 cells from 5 slices from 2 animals) cerebellum. *** indicates significantly different, $P < 0.001$. **e-f.** Confocally acquired images of immunocytochemistry for nNOS (red), GAD 65/67 (green) and nuclear stain Hoechst (blue) in the granule cell layer of SDR (**e**) and B6 (**f**) cerebellum. White arrows point to the cell body of a Golgi cell in each figure. **g.** Plot of mean ratio of fluorescence emission intensity for nNOS staining versus GAD 65/67 staining in individual Golgi cells in SDR (white, n = 6 slices), B6 (black, n = 6), and D2 (gray, n = 7,

each from 2 animals) cerebellum (ratio in B6 = 0.82 ± 0.04, n = 6 SDR = 2.05 ± 0.10, D2 = 1.65 ± 0.14) *** $P < 0.001$ by unpaired t-tests. **h-j.** Representative recordings showing increase in tonic $GABA_AR$ current and sIPSC frequency induced by NOS substrate inhibitor, L-NMMA (200μM), in SDR (**h**), B6 (**i**) and D2 (**j**) GCs. **k,l.** Plots of mean increase in sIPSC frequency (**k**) and tonic $GABA_AR$ current magnitude (**l**) induced by L-NMMA (200μM) in SDR (white; n = 16 cells), B6 (black; n = 11), and D2 (gray; n = 17) GCs. * $P < 0.05$ by Mann-Whitney U tests.

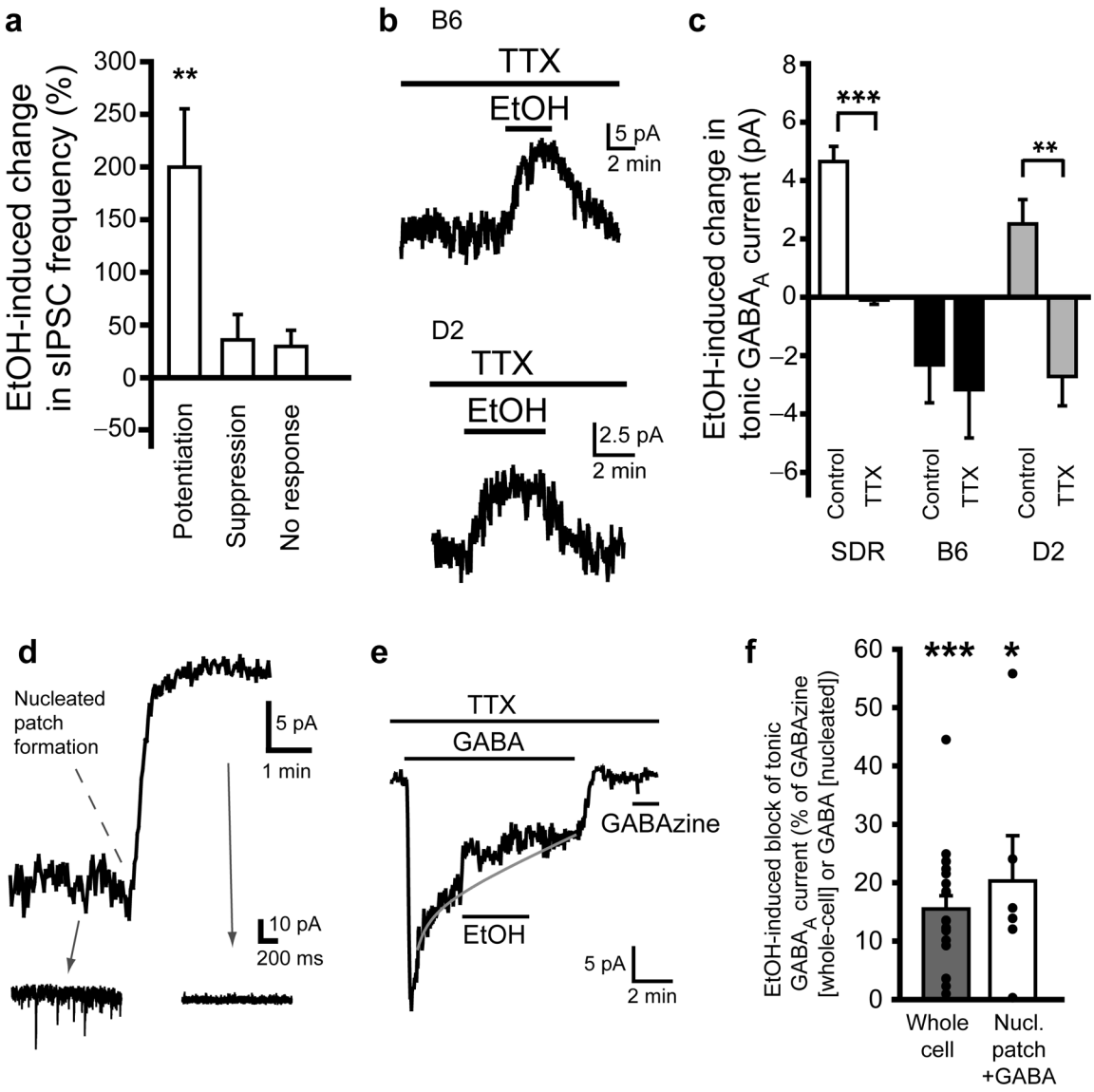

Figure 7.

EtOH-induced suppression of tonic GABA$_A$R current in B6 and D2 GCs is due to direct action on GABA$_A$Rs. **a.** Plot of mean EtOH-induced change in sIPSC frequency in B6 GCs that exhibited EtOH-induced potentiation, suppression or no change of tonic GABA$_A$R current. $^{**}P < .01$ by one-sample *t*-tests. **b.** Representative recordings showing that EtOH-induced suppression of tonic GABA$_A$R current in B6 (**top**) or D2 (**bottom**) GCs is not prevented by blocking action potential dependent release of GABA with TTX (500nM). **c.** Plot of mean EtOH-induced change in tonic GABA$_A$R current under control conditions or in TTX (500nM) shows that TTX abolishes responses to EtOH in SDR GCs (white; $n = 47$ cells for control, $n = 11$ for TTX, $^{***}P < .001$), has no effect on responses to EtOH in B6 GCs (black; $n = 39$ for control, $n = 10$ for TTX, $P = .76$) and converts mean response to EtOH from potentiation to suppression in D2 GCs (gray; $n = 31$ for control, $n = 9$ for TTX,

P = .003, by unpaired t-tests). **d. Representative trace showing GC holding current during whole-cell recording configuration and upon transition to nucleated-patch recording configuration. Note loss of tonic $GABA_AR$ current and sIPSCs (insets) upon excision of the nucleated patch from the slice. **e.** Representative trace showing a nucleated patch recording from a B6 GC in the presence of TTX, during application of exogenous GABA (100nM) and subsequently EtOH (52mM), which suppresses the exogenous GABA evoked current. Note, after wash of exogenous GABA, subsequent application of the $GABA_AR$ antagonist, GABAzine (10μM) does not generate any current, confirming that the nucleated patch is isolated from endogenous sources of GABA from the slice. **f.** Plot of mean percent block by EtOH of tonic $GABA_AR$ currents in whole cell recordings (black, n = 20 cells, ***P < .001) and of currents evoked by exogenous GABA applied to nucleated patches (white, n = 6, *P = .047. All data from B6 GCs.

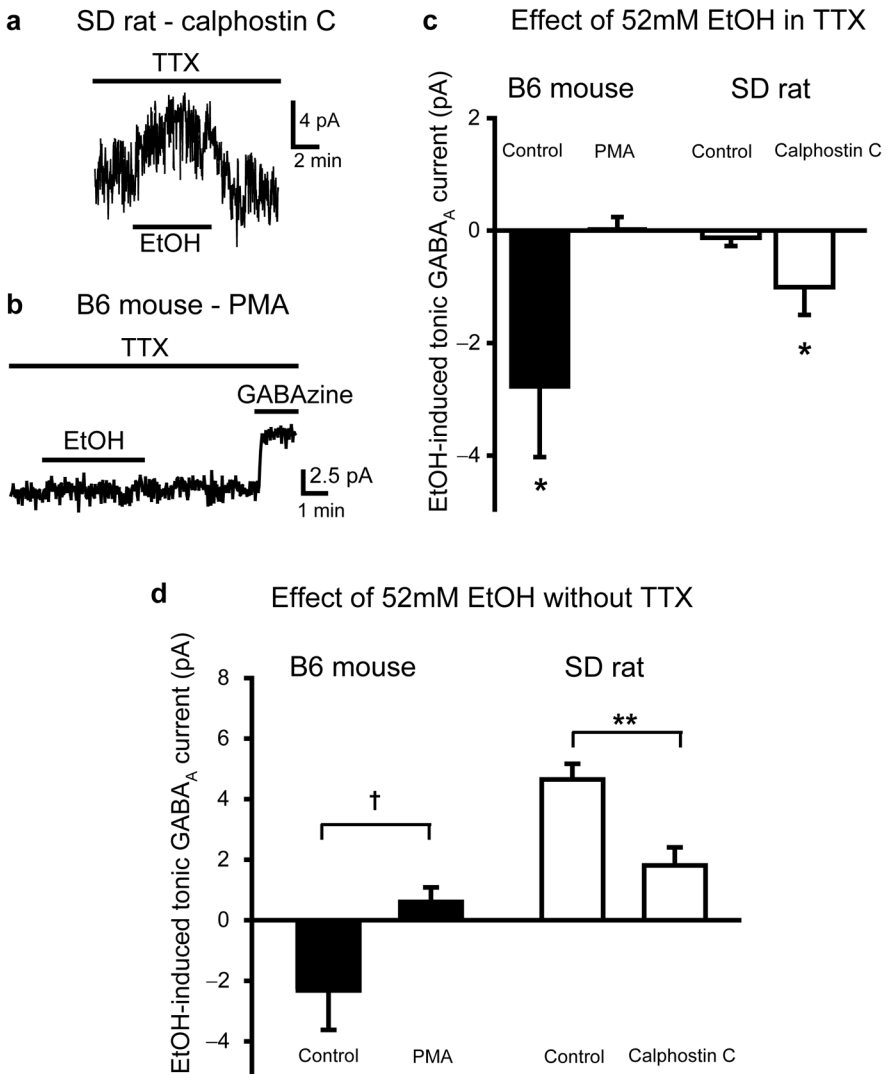

Figure 8.

Direct suppression of tonic $GABA_AR$ current by EtOH is prevented by postsynaptic PKC activity. **a**. Representative recording from an SDR GC showing that in the presence of TTX (500nM) in the bath, and PKC inhibitor, Calphostin C (100 nM), in the recording electrode, EtOH suppresses the tonic $GABA_AR$ current. **b.** Representative recording from a B6 GC showing that in the presence of TTX (500nM) in the bath, and PKC activator, PMA (100 nM), in the recording electrode, EtOH does not suppress the tonic GAB_AR current. **c.** Plot of mean EtOH-induced change in tonic $GABA_AR$ current in the presence of TTX (500nM), in B6 GCs (black) with (n = 13 cells) or without (n = 8) PMA in the recording electrode, and in SDR GCs (white) with (n = 20) or without (n = 11) Calphostin C in the recording electrode. * indicates significantly different from baseline, *$P < 0.05$ by one-sample t-tests. **d.** Plot of mean EtOH-induced change in tonic $GABA_AR$ current in normal ACSF (no TTX added), in B6 GCs (black) with (n = 6 cells) or without (n = 39) PMA in the recording electrode, in

SDR GCs (white) with (n = 16) or without (n = 47) Calphostin C in the recording electrode. **P = .003, † = .089, by Mann-Whitney U tests.